Cell Reports

Article

Dietary spermidine improves cognitive function

Graphical abstract

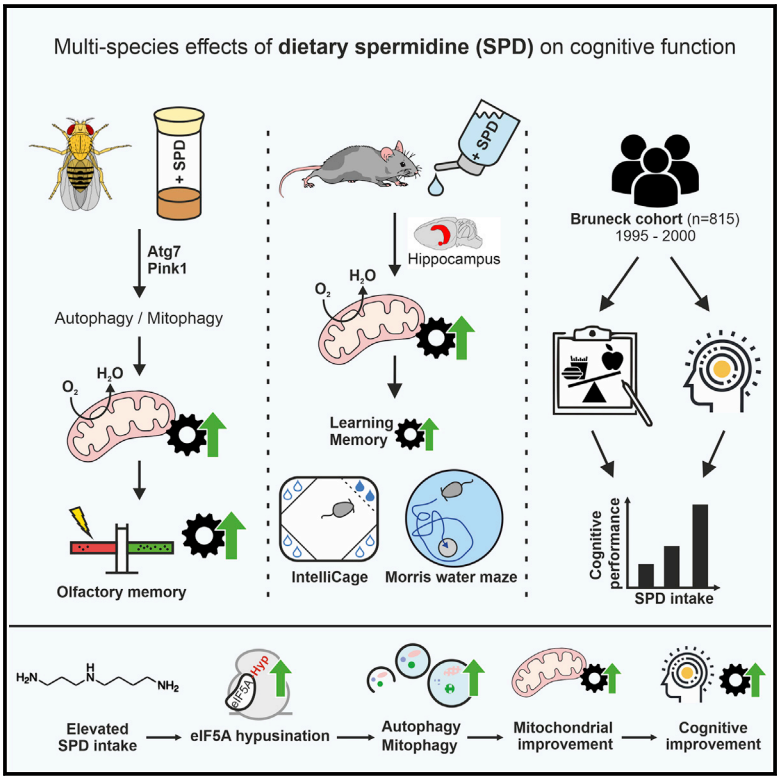

Highlights

- Elevated spermidine intake improves cognitive function in flies and mice
- Dietary spermidine intake correlates with cognitive performance in humans
- Spermidine increases mitochondrial respiration in neuronal tissue of flies and mice
- Impaired auto/mitophagy abolishes the effects on mitochondria and memory in flies

Authors

Sabrina Schroeder, Sebastian J. Hofer, Andreas Zimmermann, ..., Stefan Kiechl, Tobias Eisenberg, Frank Madeo

Correspondence

stefan.kiechl@i-med.ac.at (S.K.), tobias.eisenberg@uni-graz.at (T.E.), frank.madeo@uni-graz.at (F.M.)

In brief

Schroeder et al. report on the beneficial effects of dietary spermidine intake on cognitive performance in flies, mice, and humans. They link the polyamine's effects to elevated mitochondrial function in neuronal tissue, which depends on functional autophagy (Atg7) and mitophagy (Pink1).

Schroeder et al., 2021, Cell Reports *35*, 108985
April 13, 2021
https://doi.org/10.1016/j.celrep.2021.108985

CellPress

Cell Reports

CellPress
OPEN ACCESS

Article

Dietary spermidine improves cognitive function

Sabrina Schroeder,[1,2,29] Sebastian J. Hofer,[1,2,3,29] Andreas Zimmermann,[1,3,29] Raimund Pechlaner,[4,29] Christopher Dammbrueck,[1] Tobias Pendl,[1] G. Mark Marcello,[5] Viktoria Pogatschnigg,[1] Martina Bergmann,[1] Melanie Müller,[1] Verena Gschiel,[1] Selena Ristic,[1] Jelena Tadic,[1,3] Keiko Iwata,[6,7,28] Gesa Richter,[8] Aitak Farzi,[9] Muammer Üçal,[10] Ute Schäfer,[10] Michael Poglitsch,[1] Philipp Royer,[1] Ronald Mekis,[1] Marlene Agreiter,[1] Regine C. Tölle,[11] Péter Sótonyi,[5] Johann Willeit,[4] Barbara Mairhofer,[12] Helga Niederkofler,[12] Irmgard Pallhuber,[12] Gregorio Rungger,[13]

(Author list continued on next page)

[1]Institute of Molecular Biosciences, NAWI Graz, University of Graz, 8010 Graz, Austria
[2]BioTechMed-Graz, 8010 Graz, Austria
[3]Field of Excellence BioHealth, University of Graz, 8010 Graz, Austria
[4]Department of Neurology, Medical University of Innsbruck, 6020 Innsbruck, Austria
[5]Department of Anatomy and Histology, University of Veterinary Medicine Budapest, 1078 Budapest, Hungary
[6]Veneto Institute of Molecular Medicine, 35129 Padova, Italy
[7]Research Center for Child Mental Development, University of Fukui, 910-1193 Fukui, Japan
[8]Gottfried Schatz Research Center for Cell Signaling, Metabolism and Aging Molecular Biology and Biochemistry Medical University of Graz, 8010 Graz, Austria
[9]Otto Loewi Research Center (for Vascular Biology, Immunology and Inflammation), Division of Pharmacology, Medical University of Graz (MUG), 8010 Graz, Austria
[10]Department of Neurosurgery, RU Experimental Neurotraumatology, Medical University Graz, 8036 Graz, Austria
[11]Department of Biology, University of Fribourg, Chemin du Musée 10, 1700 Fribourg, Switzerland
[12]Department of Psychiatry, Bruneck Hospital, 39031 Bruneck, Italy
[13]Department of Neurology, Bruneck Hospital, 39031 Bruneck, Italy
[14]Department of Internal Medicine I, Gastroenterology, Hepatology, Endocrinology and Metabolism, Medical University of Innsbruck, 6020 Innsbruck, Austria
[15]Department of Psychiatry, Psychotherapy and Psychosomatics, Medical University of Innsbruck, 6020 Innsbruck, Austria
[16]Department of Psychiatry and Psychotherapy A, Hall State Hospital, 6060 Hall in Tirol, Austria
[17]HEALTH-Institute for Biomedicine and Health Sciences, Joanneum Research Forschungsgesellschaft mbH, 8010 Graz, Austria
[18]Division of Endocrinology and Diabetology, Department of Internal Medicine, Medical University of Graz, 8036 Graz, Austria

(Affiliations continued on next page)

SUMMARY

Decreased cognitive performance is a hallmark of brain aging, but the underlying mechanisms and potential therapeutic avenues remain poorly understood. Recent studies have revealed health-protective and lifespan-extending effects of dietary spermidine, a natural autophagy-promoting polyamine. Here, we show that dietary spermidine passes the blood-brain barrier in mice and increases hippocampal eIF5A hypusination and mitochondrial function. Spermidine feeding in aged mice affects behavior in homecage environment tasks, improves spatial learning, and increases hippocampal respiratory competence. In a *Drosophila* aging model, spermidine boosts mitochondrial respiratory capacity, an effect that requires the autophagy regulator Atg7 and the mitophagy mediators Parkin and Pink1. Neuron-specific *Pink1* knockdown abolishes spermidine-induced improvement of olfactory associative learning. This suggests that the maintenance of mitochondrial and autophagic function is essential for enhanced cognition by spermidine feeding. Finally, we show large-scale prospective data linking higher dietary spermidine intake with a reduced risk for cognitive impairment in humans.

INTRODUCTION

Aging is accompanied by a progressive decline in brain function (Murman, 2015), which often manifests in hippocampus-associated cognitive impairments (Todorova and Blokland, 2017). Age-associated alterations in memory formation have been linked to mitochondrial dysfunction (Todorova and Blokland, 2017). In fact, mitochondrial function is fundamental for neurotransmission and plasticity in the CNS (Kann and Kovács, 2007). In aged rodents and flies, mitochondria tend to increase in size and lose functionality, which may in part result from the loss of mitochondrial quality control (Haddadi et al., 2014; Navarro and Boveris, 2007; Srivastava, 2017). At the molecular level, aging reduces the function of respiratory complexes and oxidative phosphorylation (OXPHOS) capacity (Navarro and Boveris, 2007; Shetty et al., 2011). Along this line, dysfunctional

Herbert Tilg,[14] Michaela Defrancesco,[15] Josef Marksteiner,[16] Frank Sinner,[17,18] Christoph Magnes,[17] Thomas R. Pieber,[2,17,18] Peter Holzer,[9] Guido Kroemer,[19,20,21,22,23] Didac Carmona-Gutierrez,[1] Luca Scorrano,[6,28] Jörn Dengjel,[11] Tobias Madl,[2,8] Simon Sedej,[2,24,25] Stephan J. Sigrist,[26] Bence Rácz,[5] Stefan Kiechl,[4,27,30,*] Tobias Eisenberg,[1,2,3,30,*] and Frank Madeo[1,2,3,30,31,*]

[19]Equipe Labellisée par la Ligue Contre le Cancer, Université Paris Descartes, Université Paris Diderot, Université Sorbonne Paris Cité, INSERM U1138, Centre de Recherche des Cordeliers, 75006 Paris, France
[20]Metabolomics and Cell Biology Platforms, Institut Gustave Roussy, 94 805 Villejuif, France
[21]Pôle de Biologie, Hôpital Européen Georges Pompidou, AP-HP, 75015 Paris, France
[22]Suzhou Institute for Systems Biology, Chinese Academy of Sciences, 215123 Suzhou, China
[23]Department of Women's and Children's Health, Karolinska University Hospital, 171 77 Stockholm, Sweden
[24]Department of Cardiology, Medical University of Graz, 8036 Graz, Austria
[25]Faculty of Medicine, University of Maribor, 2000 Maribor, Slovenia
[26]Institute of Biology/Genetics, Freie Universität Berlin, 14195 Berlin, Germany
[27]VASCage, Research Centre on Vascular Ageing and Stroke, 6020 Innsbruck, Austria
[28]Department of Biology, University of Padova, 35121 Padova, Italy
[29]These authors contributed equally
[30]These authors contributed equally
[31]Lead contact
*Correspondence: stefan.kiechl@i-med.ac.at (S.K.), tobias.eisenberg@uni-graz.at (T.E.), frank.madeo@uni-graz.at (F.M.)
https://doi.org/10.1016/j.celrep.2021.108985

mitochondria contribute to the pathogenesis of age-related neurodegenerative disorders (Srivastava, 2017). As such, cognitive impairment may correlate with mitochondrial dysfunction during aging.

Mitochondrial quality control is in part maintained through autophagy, an intracellular, cytoprotective degradation mechanism, in which protein aggregates or damaged organelles are engulfed by membranous structures and fused with lysosomes for content degradation (Yorimitsu and Klionsky, 2005). Autophagy is essential for cerebral function *in vivo*, because loss of the autophagy-related proteins ATG5 and ATG7 in neurons provokes premature death and neurodegeneration in mice (Hara et al., 2006; Komatsu et al., 2006). Importantly, the capacity of the autophagic machinery progressively decreases during the course of aging (Ott et al., 2016).

Spermidine (SPD), a natural autophagy-promoting polyamine, extends lifespan across species in an autophagy-dependent manner (Eisenberg et al., 2009, 2016; Morselli et al., 2011; Wang et al., 2012). We have shown that in murine cardiomyocytes, dietary SPD induces mitophagy, a selective autophagy subroutine that targets damaged and potentially harmful mitochondria, and improves mitochondrial abundance and respiration (Eisenberg et al., 2016). Also, dietary supplementation of SPD suppresses age-induced memory impairment (AMI) and preserves synaptic flexibility in flies (Gupta et al., 2013, 2016). Moreover, intraperitoneal or intracerebral injections of SPD in rodents acutely enhance cognitive performance in different tasks, which has been ascribed to the action of SPD toward *N*-methyl-D-aspartate (NMDA) receptors (Guerra et al., 2016). Intraperitoneal SPD injections also restore memory capacity in mouse models of mild cognitive impairment, an effect that is abolished when co-administering the autophagy inhibitor 3-methyladenine (De Risi et al., 2020). Although these findings provide important insight into the molecular mechanism of SPD, the translatability of polyamine injections to humans is poor. Moreover, it is unclear whether the more feasible strategy of dietary SPD supplementation is able to improve behavioral, neuronal, and cognitive aspects during normal aging as to date, no comprehensive study addressing this question has been performed.

Here, we show that late-in-life dietary SPD supplementation improves cognitive function in aged mice. Dietary SPD has direct molecular effects in the hippocampus and enhances its respiratory capacity. In flies, we show that SPD-enhanced respiration requires functional autophagy and, specifically, the mitophagy mediators Pink1 and Parkin. In line with that, improved memory performance upon SPD feeding depends on neuronal Pink1. Finally, in a prospective cohort study, we demonstrate that higher nutritional SPD intake is associated with a lower risk for cognitive impairment and decline in humans.

RESULTS AND DISCUSSION

Dietary SPD passes the blood-brain barrier and improves spatial and temporal memory in aged mice

We previously reported neuroprotective effects of SPD administration on cognitive function in fly models of aging (Gupta et al., 2013) and neurodegeneration (Büttner et al., 2014). However, the impact of chronic nutritional SPD supplementation on cognition during physiological aging in mammals has never been investigated.

To address this, we first determined if orally supplemented SPD can pass the blood-brain barrier (BBB). We fed 18-month-old C57BL/6J male mice deuterium-labeled (d8)-SPD via drinking water. We found that orally supplied SPD was detectable in brain tissue of aged mice after 1 week and increased in a time-dependent manner after 4 and 8 weeks of feeding to a level of up to 30% of circulating levels (Figure 1A). The relatively slow kinetics of SPD uptake in the brain is in agreement with previous studies in rats after acute systemic injection of spermidine (Guerra et al., 2016; Shin et al., 1985). Importantly, small amounts (in the range of nmol) of SPD injected into specific brain regions in rats have been shown to improve cognitive function, more specifically memory acquisition and fear conditioning in shock-motivated tasks (Guerra et al., 2016), while repeated SPD injections can improve social memory (Mikolajczak et al., 2002).

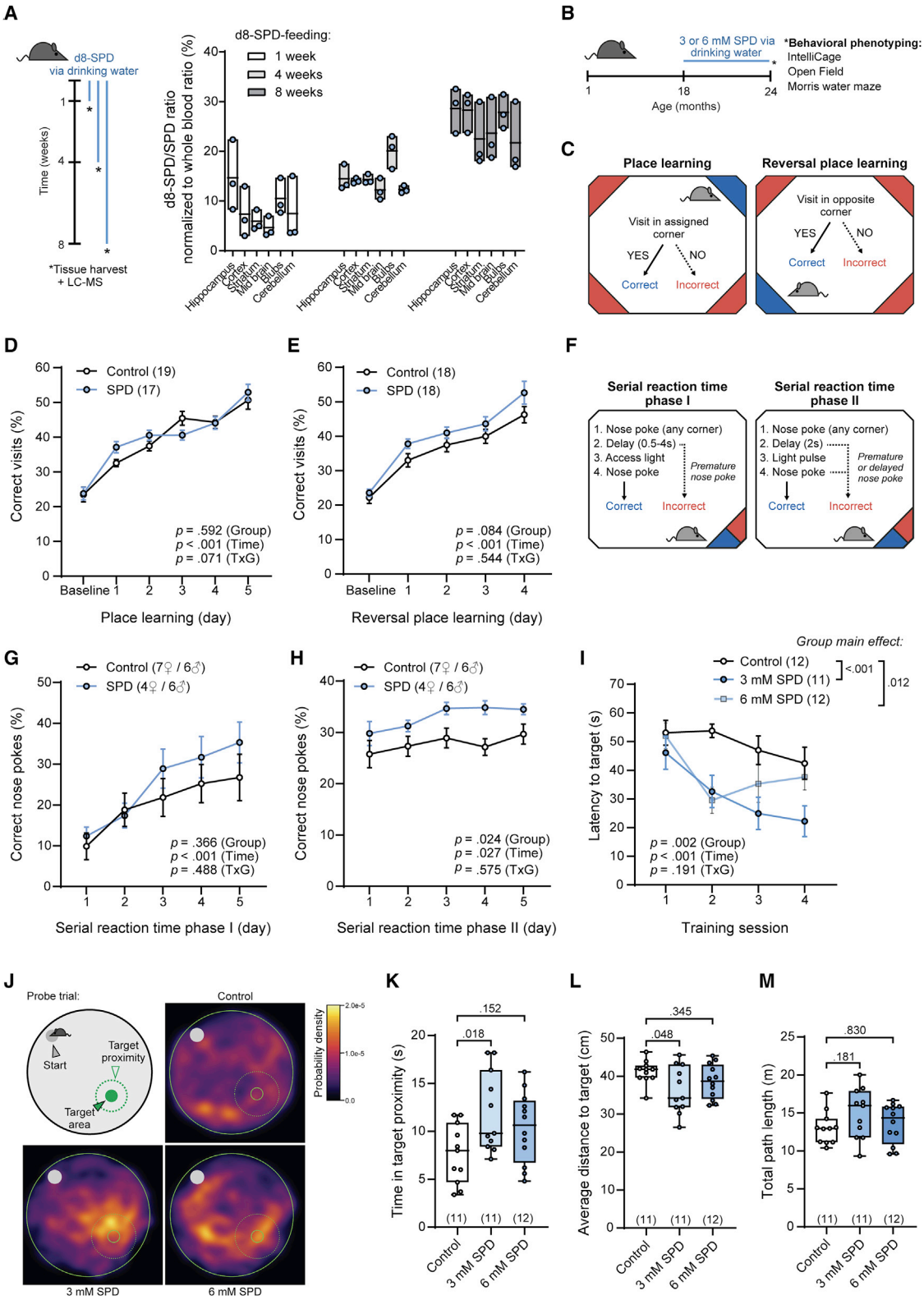

Figure 1. Dietary spermidine reaches brain tissue and improves cognition in aged mice

18-month-old C57BL/6J male (or female as indicated) mice were supplemented with 3 or 6 mM spermidine (SPD) in the drinking water. Age-matched untreated animals served as control. Numbers in brackets indicate the number of animals per group.

(legend continued on next page)

We next assessed whether dietary SPD induces detectable molecular changes in cerebral tissue in aged mice. Explorative analysis of the proteomic profile (>5,000 proteins identified) of brains from aged control and SPD-fed mice revealed 55 proteins that differed between the two groups (fold change > 2 or < 0.5) (Figure S1A), of which 5 were significantly different (Student's t test $p < 0.05$) (Figures S1A and S1B).

We next compared the cognitive performance of aged, 24-month-old mice supplemented with SPD for 6 months in a battery of cognitive and behavioral tests (Figure 1B). First, we used the IntelliCage system (Robinson and Riedel, 2014), which allows automated monitoring of cognitive performance in a largely researcher-independent homecage environment. We performed an adapted testing schedule as previously described (Mechan et al., 2009) to measure hippocampus-dependent cognitive capacity (Figure 1C). The schedule consists of three phases: habituation, place learning (PL), and reversal PL (rPL). The first phase allowed unlimited access to food and drinking water. Overall, both groups adapted quickly to the new environment. Explorative behavior declined (Figure S2A) and visit duration (Figure S2B), as well as the number of licks per visit (Figure S2C), increased over time, indicating the comprehension of the cage layout. Subtle changes regarding the general behavior (Figures S2A and S2B) were detected, showing significantly shorter visit durations in the SPD group (Figure S2B). Drinking behavior remained largely unchanged (Figures S2D and S2E). However, the number of licks per visit differed over time in the SPD group (Figure S2C), which is consistent with the shorter visit duration. Altogether, these results indicate that SPD slightly altered spontaneous behavior and/or exploration patterns in aged mice. This was confirmed in an open field test, where SPD-fed animals showed a slight increase in the time spent in the central area and reduced latency to center (Figures S2F–S2I).

Next, we tested spatial learning capacity. During the PL and rPL phases, animals were restricted to access one out of four individually assigned corners for drinking within two one hour time intervals (Figure 1C). At baseline, both groups showed comparable numbers of correct visits. Curve comparison showed that both SPD-fed and age-matched control animals were capable of learning the task within the given time frame (Figure 1D). After 1 day, SPD-fed animals showed 37.1% (95% confidence interval [CI]: 33.7–40.5) correct visits versus 32.6% (95% CI: 30.4–34.7) correct visits of control mice; however, this effect did not persist at later days, leading to a non-significant group main effect ($p = 0.592$) and non-significant group × time interaction ($p = 0.071$) overall. In the rPL phase, where corners were reassigned diagonally, SPD-fed and control mice again performed comparably (group main effect: $p = 0.084$) (Figure 1E). Overall, the percentage of correct corner visits matches those of previously reported aged cohorts using similar protocols (Mechan et al., 2009).

We next decided to employ more complex assays, moving to cognitive domains of "attention" and "impulsivity" that may better unmask age-induced cognitive impairments (Figure 1F). Aged animals (both males and females in separate runs) were subjected to serial reaction time (SRT) tasks, which required the animals to learn the association between light-emitting diode (LED) lights and water access. In the first task (SRT I), mice started trials by an initial "nose poke" (NP) and had to wait a random interval of 0.5–4 s for a subsequent 2-s light stimulus, which indicated that they could open the door by another NP. Premature NPs before the LEDs were lit were counted as incorrect, upon which the animals had to leave the corner to restart the trial. Overall, aged animals were capable of learning the presented task without any statistically significant group effect in this test phase (Figure 1G). In the second SRT task (SRT II), trials were again started by initial NPs. However, the animals could not open the doors until a short, randomly assigned light pulse flashed for 0.2–1 s, which started 2 s ("limited hold") after starting the trial and which indicated a 2-s reaction window. NPs before the light pulse and after the limited hold were counted as incorrect and forced the animals to leave the corners before they could start another trial. In this second test phase (SRT II), SPD-treated animals showed a significant overall improved performance (group main effect: $p = 0.024$) (Figure 1H). In sum, late-in-life SPD feeding led to changes in explorative behavior and slightly improved performance in homecage environment tasks.

We next decided to strengthen these results in a forced learning setup. We therefore employed Morris water maze (MWM), a well-established and robust assay for measuring spatial learning and memory deficits in aging (Kennard, 2011). MWM tests the ability of mice to navigate in a swimming area in three phases: (1) adaptation to the swimming pool and finding a visible platform; (2) spatial acquisition phase, in which mice

(A) Deuterium-labeled (dietary) SPD (d8-SPD) detected in different brain areas. Data show the d8-SPD/SPD ratios (dietary/endogenous SPD) normalized to circulating (whole blood) ratios after 1, 4, and 8 weeks of feeding, n = 3 animals. Data are shown as minimum-maximum (min-max) boxplots with line at mean.
(B) Setup for late-in-life SPD supplementation. Animals were randomly assigned to groups at 18 months of age and tested in different behavior assays after 6 months of feeding: IntelliCage place learning (PL), reversal place learning (rPL), serial reaction time (SRT) and Morris water maze (MWM).
(C–H) IntelliCage behavioral testing of 24-month-old mice, supplemented with 3 mM SPD for 6 months.
(C) Setup for PL and rPL.
(D and E) Correct corner visits over a course of 4–5 days during PL (D) or rPL (E). Data show means ± SEM.
(F) IntelliCage setup for serial reaction time phases I and II.
(G and H) Correct nose pokes over a course of 4–5 days during serial reaction time phase I (G) or phase II (H). Data show means ± SEM.
(I–M) MWM behavioral testing of 24-month-old mice, supplemented with 3 or 6 mM SPD for 6 months.
(I) Latency to target from north starting point during training phase. Data show means ± SEM.
(J) Heatmaps showing mean probability density during probe trial.
(K–M) Time spent in target proximity during probe trial (K), average distance to target (L), and total path length (M).
Boxplots represent interquartile range (IQR; line at median) and whiskers show min-max range. Statistical significance in (D), (E), (G)–(I) was assessed by a repeated measures (RM) mixed-model ANOVA. Statistical significance in (K)–(M) was assessed by ANOVA with comparisons with control and Dunnett's multiple comparison correction.

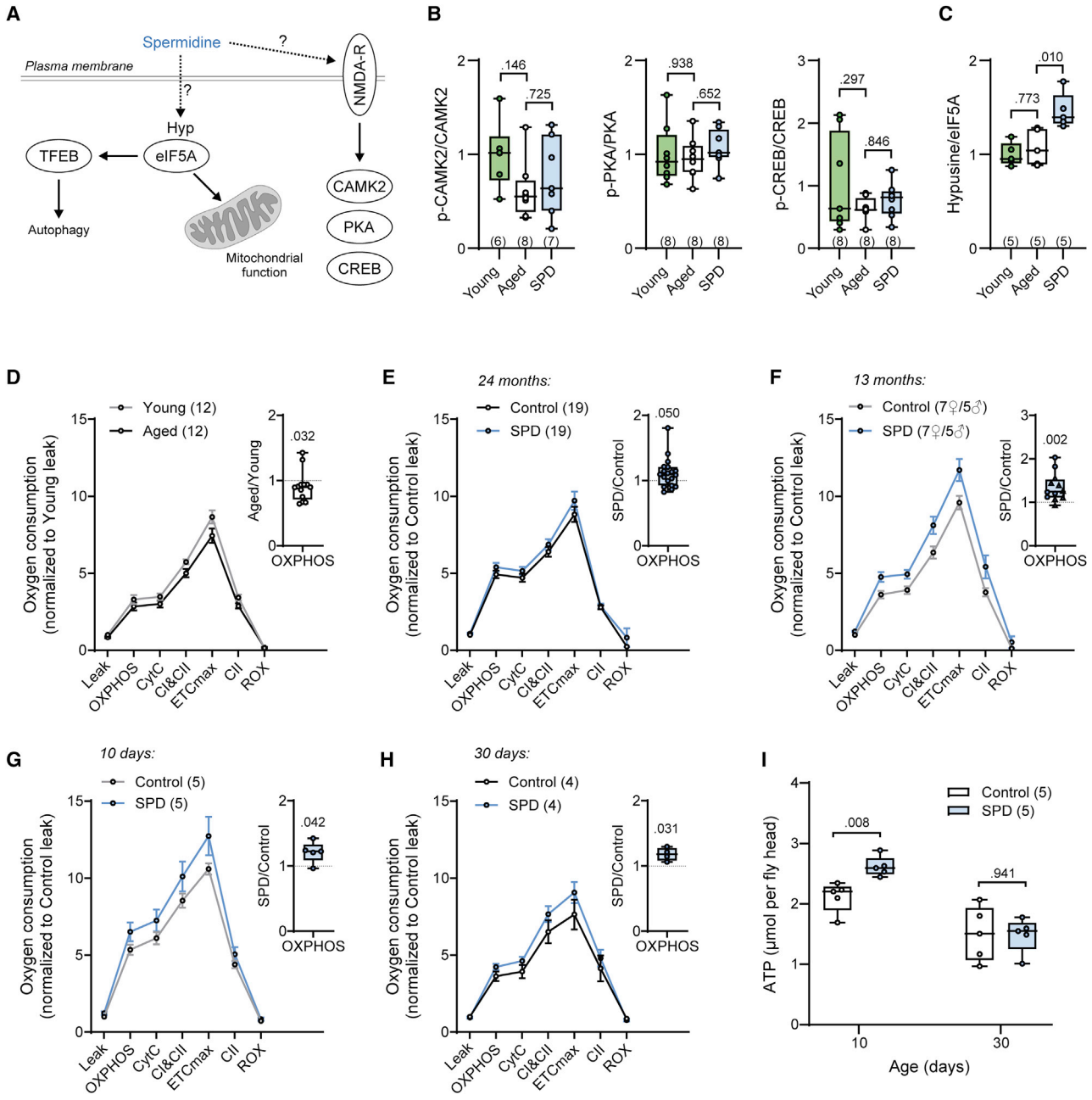

Figure 2. Dietary SPD improves mitochondrial respiratory competence in aged mice and flies

C57BL/6J male (or female as indicated) mice were supplemented with 3 mM SPD in the drinking water for 5–6 months. Age-matched untreated animals served as control. Numbers in brackets indicate the number of animals per group in (B)–(F) and number of experiments in (G) and (H).

(A) Schematic overview of proposed molecular effects of SPD.

(B and C) Hippocampal levels of PKA, CREB, and CaMKII phosphorylation (B) and eIF5A hypusination (C). Boxplots represent IQR (line at median) and whiskers show min-max range. Statistical significance was assessed by ANOVA with post hoc Tukey's test.

(D–F) Oxygen consumption of hippocampal extracts upon SPD supplementation at different life stages, assessed by high-resolution respirometry. Curves show oxygen consumption per microgram protein normalized to leak levels of the respective control condition, and insets represent pairwise ratios of the oxygen consumption during ADP-coupled respiration (OXPHOS).

(D) Hippocampal respiration in young (5–9 months) and aged (24 months) animals, normalized to young leak levels.

(E) Hippocampal respiration upon SPD supplementation late-in-life (18–24 months), normalized to control leak levels.

(F) Hippocampal respiration upon SPD supplementation in middle-aged animals (9–13 months), normalized to control leak levels.

(G and H) Oxygen consumption of head extracts from female w^{1118} flies fed with 2 mM SPD for 10 or 30 days compared with respective controls. Curves show oxygen consumption per microgram protein normalized to leak levels of the respective control condition, and insets represent pairwise ratios of the oxygen

(legend continued on next page)

have to navigate to the submerged (but still present) platform within 60 s; and (3) spatial retrieving phase (i.e., probe trial), where the platform has been removed and mice try to recall spatial information of where the platform used to be (Figure S3A). We also included a cohort fed with 6 mM SPD to examine whether doubling the supplemented intake resulted in further improved learning and memory abilities. During the 4-day acquisition phase, all groups learned the task as indicated by a time-dependent reduction in latency to target (Figure 1I). Mice fed with 3 mM SPD showed significantly reduced latency to target compared with controls (Bonferroni-corrected group main effect: $p < 0.001$), whereas mice fed with 6 mM SPD only initially performed better than control animals (Figure 1I). In the last training session, 58% of control mice, 91% of 3 mM SPD-fed mice, and 75% of 6 mM SPD-fed mice successfully completed the task (i.e., finding the platform within 60 s), suggesting that SPD improved general perception and/or capabilities to cope with the task (Figure S3B). This improved learning ability was also reflected in the spatial retrieving phase, where 3 mM SPD-fed mice showed an increased time spent in target proximity (Figures 1J and 1K) and a significantly reduced average distance to target compared with control animals, indicating a more direct path to the platform position (Figure 1L), while the overall path length was similar to controls (Figure 1M).

Mice fed 6 mM SPD exhibited only small, statistically non-significant improvements compared with controls during the probe trial (Figures 1J–1M) and also showed a different target-finding strategy compared with mice fed 3 mM SPD (Figure 1J). This may argue for transition to adverse effects of chronically applied SPD at very high doses. High-dose SPD supplementation (30 mM for 30 days) was previously reported to elicit maladaptive effects on muscle strength, which was attributed to excessive autophagy activation (Chrisam et al., 2015).

In female mice, late-in-life SPD feeding at both 3 and 6 mM did not improve MWM performance (Figures S3C–S3H), which may be because of superior learning capabilities compared with males and possibly missing age deficits (female mice reduced latency to target from 50 to 20 s within four learning sessions). It will thus be interesting and important to test an advanced age and possibly also lower doses of spermidine in females.

Taken together, late-in-life dietary SPD supplementation increased the performance of aged male mice in two spatial learning tasks. Our results highlight the need for more detailed dose-response studies, testing also lower SPD doses and potential sex specificity.

SPD enhances hippocampal mitochondrial respiration capacity

Given the cognitive improvements by dietary SPD, we aimed at elucidating the underlying molecular mechanism. SPD reportedly activates NMDA receptors and downstream targets (Figure 2A), especially when administered by injection (Guerra et al., 2016). However, our feeding setup did not coincide with persistent activation of known NMDA receptor targets, such as protein kinase A (PKA), cAMP response element-binding protein (CREB), or Ca^{2+}/calmodulin-dependent protein kinase II (CaMKII) (Figures 2B and S4C). A recently proposed direct mechanism of SPD is through hypusination of the eukaryotic translation initiation factor 5A (eIF5A), which improves translation of the autophagy regulator TFEB, as well as mitochondrial proteins in T/B lymphocytes (Puleston et al., 2019; Zhang et al., 2019) (Figure 2A). Indeed, dietary supplementation of SPD increased hypusination levels also in hippocampi of aged mice, while overall eIF5A and also TFEB protein levels were not altered significantly (Figure 2C; Figures S4A, S4B, and S4D).

Mitochondria are critically implicated in the progression of brain aging (Grimm and Eckert, 2017; Sun et al., 2016). Given the observed effects of dietary SPD on hypusination in the hippocampus, and our previous observations that SPD protects from age-related synaptic alterations, including mitochondrial parameters at hippocampal mossy fiber synapses (Maglione et al., 2019), we asked whether mitochondria-dependent processes may underly cognitive improvements elicited by SPD. We previously showed that SPD supplementation improves mitochondrial function in cardiomyocytes of aged mice in an autophagy-dependent manner (Eisenberg et al., 2016). Therefore, we tested, by using high-resolution respirometry, whether SPD might provoke functional mitochondrial improvements in the hippocampus of SPD-fed mice. Hippocampal homogenates from aged mice showed an age-associated decline in OXPHOS capacity compared with young individuals (Figure 2D, OXPHOS state shown in insets), while samples from SPD-treated animals showed a trend ($p = 0.0497$) toward higher OXPHOS capacity (Figure 2E). To test whether SPD preserved respiration during aging or generally enhanced respiratory capacity independent of age, we analyzed SPD-induced changes in young (5-month-old) and middle-aged (13-month-old) mice after 3- and 5-month feeding, respectively. Interestingly, middle-aged mice fed with SPD showed a more pronounced improvement in respiratory competence compared with controls (Figure 2F). At 13 months of age, no age-related decline of respiration was detectable (Figure S5A), favoring the idea that SPD rather generally boosts respiratory competence than it counteracts an age-associated decay of mitochondrial function. However, SPD failed to improve respiratory capacity in young animals after 3 months of feeding (Figure S5B), arguing that susceptibility of animals toward SPD's effect on respiration may depend on timing and/or age. One possible explanation would be a failure of SPD to pass the BBB in young animals, although this hypothesis requires future testing. Altogether, SPD intake promoted hippocampal mitochondrial function in aged, but not young, mice. In line, chronic SPD feeding in SAMP8 mice, an accelerated aging model (Xu et al., 2020), increased mitochondrial protein levels and

consumption during ADP-coupled respiration (OXPHOS). Oxygen consumption normalized to control leak levels. Curve data in (D)–(H) represent means ± SEM, while insets boxplots represent IQR (line at median) and whiskers show min-max range of pairwise calculated ratios during OXPHOS.

(I) ATP content in head extracts from female w^{1118} flies fed with 2 mM SPD for 10 or 30 days compared with respective controls. Boxplots represent IQR (line at median), and whiskers show min-max range.

Statistical significance in (B) and (C) was assessed by ANOVA with Tukey's multiple comparison tests, in (D)–(H) with ratio paired t tests, and in (I) with an unpaired t test.

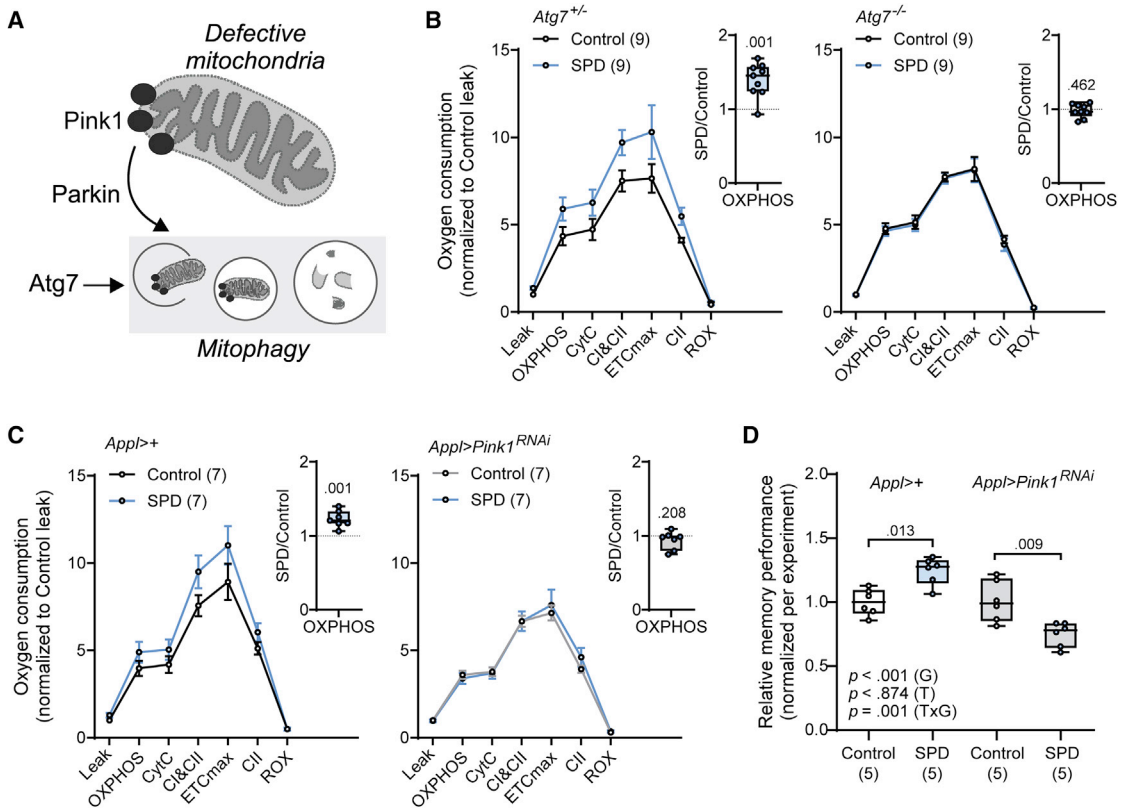

Figure 3. SPD-mediated mitochondrial and cognitive improvements require PINK1-dependent quality control

(A) Schematic overview of key players in mitochondrial quality control.

(B and C) Female flies were aged with or without supplementation of 2 mM SPD for 10 (B) or 20 (C) days. Oxygen consumption of head extracts from (B) *Atg7* mutant (heterozygous $Atg7^{+/-}$ [$Atg7^{d14/d30}$] controls or homozygous knockout $Atg7^{-/-}$ [$Atg7^{d14/d77}$]) or (C) Pink1 *RNAi*-mediated knockdown animals. Curves show oxygen consumption per microgram protein normalized to leak levels of the respective control condition, and insets represent pairwise ratios of the oxygen consumption during ADP-coupled respiration (OXPHOS). Curve data in (B) and (C) represent means ± SEM, while insets boxplots represent IQR (line at median), and whiskers show min-max range of pairwise calculated ratios during OXPHOS.

(D) Olfactory, aversive intermediate-term (3 h) memory performance of male and female *Pink1* RNAi flies or corresponding controls fed with control food or food containing 5 mM SPD for 20 days. The average performance in each experiment was set to 1. Boxplots represent IQR (line at median), and whiskers show min-max range.

Statistical significance in (B) and (C) was assessed by ratio paired Student's t test within groups, and two-way ANOVA in (D) with t tests of simple main effects. The number of independent experiments is indicated in brackets.

improved cognition, supporting our observations under physiological aging conditions.

SPD supplementation delays age-related ailments across multiple species, including fruit flies (Gupta et al., 2013, 2016). To explore our findings in a mechanistic fashion, we employed the versatile genetic model *D. melanogaster*. Again, we found that head homogenates of female flies treated with SPD for 10 or 30 days exhibited enhanced O_2 consumption rates (Figures 2G and 2H). Similar effects were observed in male flies at day 10 (Figure S5C) and less pronounced at day 30 (Figure S5D). In this case, we did not detect an age-dependent decline in respiration (Figure S5E) similar to what we observed for middle-aged 13-month-old mice. Thus, the mitochondria-enhancing functions of SPD in the aging brain appear to be conserved among the tested species and partly independent of age phenotypes. This SPD-mediated increase in respiration coincided with elevated ATP levels, at least after 10 days of feeding (Figure 2I).

Autophagy is essential for SPD-mediated cerebral mitochondrial quality control

In flies, SPD-mediated protection against AMI depends on functional autophagy (Gupta et al., 2013), and autophagy *per se* has been described as crucial for mitochondrial quality control during aging and neurodegeneration (Shi et al., 2018; Zhang et al., 2018) (Figure 3A). Thus, we examined the effects of SPD on mitochondrial function in the absence of the autophagy-essential gene *Atg7*. Indeed, although SPD was still able to improve respiration in heterozygous $Atg7^{+/-}$ control mutants, the effect was completely abolished in homozygous $Atg7^{-/-}$ knockouts (Figure 3B). Of note, these homozygous knockouts showed elevated O_2 consumption rates compared with heterozygous controls (Figure S6A), which would be consistent with a general loss of autophagic degradation of mitochondria.

To further specify which autophagy subroutines might be connected to SPD-mediated mitochondrial protection, we tested for

the involvement of PTEN-induced putative kinase 1 (Pink1), which is associated with mitophagy (Cornelissen et al., 2018). Thus, we expressed *Pink1*-double-stranded hairpin RNA to downregulate the levels of Pink1 in neuronal tissue via RNAi. SPD failed to elevate respiration upon knockdown of *Pink1* (Figure 3C). Similar effects were observed in knockouts of *park* (Figure S6B), the homolog of Parkin, an E3 ubiquitin ligase associated to mitophagy, that acts downstream of Pink1 (Jin and Youle, 2012). Notably, respiration was not affected significantly by knockdown of *Pink1* or knockout of *park per se* at the ages analyzed (Figures S6C and S6D). In agreement with our findings, SPD was recently shown to mediate mitophagy by activating ATM (ataxia telangiectasia mutated), a protein involved in nuclear DNA damage repair and other signaling pathways, including mitochondrial quality control, and consequently via Pink1 regulation *in vitro* neuronal cell cultures (Qi et al., 2016). Our mechanistic data are further corroborated by a recent study exploring lifespan-prolonging effects of SPD in a worm model of neurodegeneration, which were largely dependent on the presence of PINK-1 and the *C. elegans* Parkin ortholog, PDR-1 (Yang et al., 2020).

To link the effect on mitochondrial function to cognitive performance, we measured intermediate-term aversive olfactory memory (ITM), which is reportedly improved upon SPD supplementation (Gupta et al., 2013). Although lifelong treatment with SPD improved ITM scores by 25% in controls, it did not enhance memory in neuronal *Pink1* knockdown flies and even led to diminished performance (Figure 3D; Table S1). Noteworthy, neither the control nor knockdown strains exhibited alterations by SPD in the behavioral responses to electrical shocks, used as an aversive stimulus in the ITM test, nor the preference to the odors (Table S2). In sum, SPD supplementation protects from age-related mitochondrial dysfunction and AMI in an *Atg7*- and *Pink1*/*park*-dependent manner.

The role of autophagy in learning processes is complex. For instance, the autophagy inducer rapamycin has been shown to impair memory formation and retrieval in rats (Jobim et al., 2012). In contrast, caloric restriction activates hippocampal autophagy and reduces age-associated cognitive decline (Yang et al., 2014). Reduced autophagic capacity in the hippocampus was shown to centrally contribute to cognitive dysfunction during murine aging (Yang et al., 2014), supporting a beneficial role of autophagy during neuronal aging. Moreover, the stimulation of memory processes itself promotes autophagy, while inhibition of autophagy prevents formation of new memory and functioning synaptic plasticity in mice (Glatigny et al., 2019). Restoring autophagy to pre-aged levels in the hippocampus is sufficient to ameliorate age-impaired memory deficits (Glatigny et al., 2019). The same findings hold true for flies, putting autophagy at the nexus of memory function and aging (Bhukel et al., 2019). Altogether, in combination with the well-studied autophagy-inducing effects of SPD, these data corroborate our findings that the autophagy inducer SPD can improve the performance of aging animals.

Higher nutritional SPD intake correlates with enhanced cognition in humans

Encouraged by the results from model organisms, we evaluated possible correlations of dietary SPD intake (assessed from food frequency questionnaires [FFQs] and calculated SPD contents in various foods [Kiechl et al., 2018]) with cognitive function and decline in humans, using data collected within the Bruneck study (Bonora et al., 2004; Kiechl and Willeit, 2019) (Figure S7). This study is one of a few prospective population-based studies with a thorough and repeated ascertainment of diet and cognitive status (Eisenberg et al., 2016; Kiechl et al., 2013, 2018; Stegemann et al., 2014; Willeit et al., 2014). SPD intake was stable over time (average correlation of SPD intake in repeated FFQ assessments, $r = 0.54$) (Kiechl et al., 2018). Baseline characteristics of the study population are shown in Table S3 ($n = 815$).

Cognitive function was assessed by quinquennial Mini-Mental State Examination (MMSE) tests, a standard screening measure of overall cognitive function in the clinical setting compared with a healthy reference population. In a linear regression analysis adjusted for age, sex, and caloric ratio, SPD intake correlated with MMSE *Z* scores in 1995 and 2000, as well as an overall score change (ΔMMSE) between the two assessment time points (Table S4). A logistic regression analysis revealed that SPD intake also reduced the odds for developing cognitive impairment, which is indicated by MMSE *Z* scores below −1.03 according to the recommendations by the Consortium to Establish a Registry for Alzheimer's Disease (CERAD) 1.0 (Morris et al., 1989; Welsh et al., 1994) (Table S4).

Baseline (1995) SPD intake was significantly related to incident cognitive impairment in 2000, assessed by the CERAD test battery. The age, sex, and caloric ratio-adjusted odds ratio (95% CI) per 1-SD unit higher SPD intake amounted to 0.63 (0.51–0.78) ($p < 0.001$) (Table S5). This analysis was confined to study participants with normal baseline (1995) cognition. Findings remained robust under multivariable adjustment and in sensitivity analyses (e.g., after exclusion of patients with major depression; Table S5). Findings were similar in men and women and consistent within different age groups and categories according to the caloric ratio (interaction $p > 0.05$; Figure 4A). Moreover, the effects remained significant irrespective of social status or level of education, although education tended to influence the effect size (interaction $p = 0.07$; Figure 4A).

When the probands were ranked into groups based on SPD intake levels (low, medium, and high intake), the risk for cognitive impairment gradually decreased across SPD tertile groups, indicating an inverse dose-response relationship (Figure 4B). Finally, SPD intake was significantly related to the cognitive CERAD domains memory and executive functioning and the cumulative impairment score (Figure 4C). The language domain also tended to be related to SPD intake ($p = 0.10$).

SPD content in food correlates with other macronutrients and dietary patterns that may modify the risk for cognitive impairment (Kiechl et al., 2018). To thoroughly account for this potential source of confounding, we further adjusted the analysis for a variety of dietary characteristics and controlled for the Alternate Healthy Eating Index (McCullough et al., 2002), which still resulted in significant associations (Table S5). In this context, it should be emphasized that SPD is contained in a large number of different foods (including bread, salad, cheese, potatoes, noodles, meat, fish, and most fruits and vegetables) and not in an extreme pattern of food items, making confounding by overall healthy diet *a priori* less likely. Collectively, our findings lend

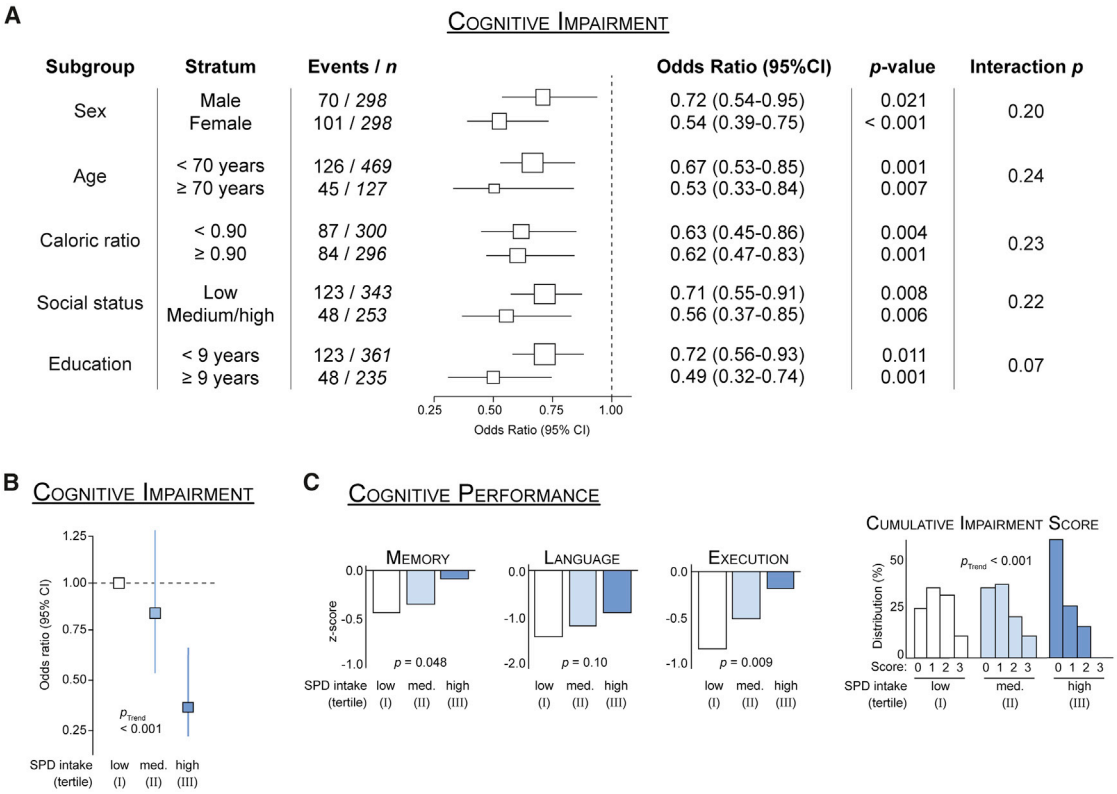

Figure 4. Nutritional SPD intake correlates with improved cognitive function in humans

(A) Odds ratios (ORs) for incident cognitive impairment (following CERAD criteria, see STAR Methods) according to nutritional SPD intake at baseline in subgroups. ORs presented are for a 1-SD higher $\log_e$-transformed calorie-adjusted SPD intake and derived from logistic regression analysis adjusted for age, sex, and caloric ratio.

(B) Inverse dose-response relationship of tertile groups of nutritional SPD intake with odds for incident cognitive impairment. SPD intake was assessed at baseline in 1995. Cognitive status was thoroughly assessed in 2000 and the analysis confined to individuals with normal baseline cognitive status in 1995. ORs presented were derived from logistic regression analyses adjusted by age, sex, and caloric ratio.

(C) Association of tertile groups of SPD intake with the three individual cognitive CERAD domains memory, language, and execution. *Z* scores represent the performance in relation to a healthy reference population from Basel (see STAR Methods) with low *Z* scores indicating more deficits. Cumulative impairment scores of 0, 1, 2, and 3 indicate *Z* scores below −1.03 (cutoff for cognitive impairment) in none, one, two, or all three cognitive domains.

p values were derived from generalized linear models adjusted for age, sex, and caloric ratio.

strong support to the concept that nutrition rich in SPD protects against cognitive impairment and decline.

Our findings meet the rules of evidence of causation (Hill's classic criteria) (Hill, 1965), including a considerable strength and dose-response type of association (Figure 4B; Table S5), consistency in subgroups and sensitivity analyses (Figure 4A; Table S5), temporality (Figure S7; Table S5), plausibility and experimental support, specificity (the key association applies to SPD, but not its metabolic precursor putrescine; data not shown), as well as coherence to SPD's lifespan-prolonging and cardioprotective effects (Eisenberg et al., 2016). Further strengths of the epidemiological data presented include the following: (1) near-complete participation and follow-up (>90%); (2) use of the extensive gold standard FFQs (Willett et al., 1985) administered by dieticians; (3) in-house validation of the FFQs against 9-day diet records; (4) prospective follow-up (Figure S7); and (5) the high standards in nutritional epidemiology applied (see STAR Methods).

Finally, the consistent effects of dietary spermidine on mitochondrial function and cognitive performance across species borders (flies, mice, humans) reported by us and other groups suggest a broad potential of the polyamine in treating cognitive disorders and warrants further interventional clinical studies. Of note, the epidemiological data reported here are further underlined by a recent study, which reported positive correlations of dietary SPD intake and hippocampal volume, as well as cortical thickness in elderly humans (Schwarz et al., 2020).

Limitations of study

Several limitations inherent to behavioral assessment during physiological aging apply to our study. First, the observed behavioral improvements by SPD feeding in mice at the late time point (24 months) are accompanied by only subtle increases of hippocampal mitochondrial respiration, which seem to be more pronounced when measured earlier in life. However, decisive changes applied in middle-aged mice may well integrate to

behavioral and physiological improvements later in life. Second, although the increase in mitochondrial respiration seems sex independent (as seen in flies and mice at the middle-aged time point), the cognitive improvements by SPD feeding in the MWM appear to occur only in male mice, which, however, also performed worse than female mice in general. We cannot rule out that there are different sex-specific kinetics underlying the relationship of SPD's mitochondrial and cognitive effects. Thus, we speculate that a more comprehensive analysis of cognitive effects in female mice could reveal enhanced cognitive function by SPD feeding for different feeding and/or testing schemes. Finally, nutritional epidemiology constraints apply to our study as well. These include measurement errors due to the subjects' self-report of diet and the non-consideration of storage conditions and food preparation for each food. These sources of variability, however, may be expected to weaken existent relationships rather than to create spurious ones.

Conclusions

The combination of epidemiological and experimental data raises the intriguing possibility that dietary SPD may be protective against cognitive decline in humans. Elevated intake of SPD has recently been shown to be safe in healthy, elderly humans (Schwarz et al., 2018). In a phase II trial including subjects with self-reported cognitive decline, SPD led to detectable improvements in cognition already after a 3-month treatment period (Wirth et al., 2018). We herein propose that dietary SPD acts in a neuroprotective manner during normal aging. The beneficial effects of SPD appear to depend on autophagy- and likely mitophagy-related processes that culminate in improved mitochondrial capacity, at least in model organisms. Accordingly, the straightforward and inexpensive availability of nutritional SPD in the human diet may provide a potent strategy to prevent the course of age-related or disease-driven cognitive decline in the general population.

STAR★METHODS

Detailed methods are provided in the online version of this paper and include the following:

SUPPLEMENTAL INFORMATION

Supplemental information can be found online at https://doi.org/10.1016/j.celrep.2021.108985.

ACKNOWLEDGMENTS

F.M. is grateful to the Austrian Science Fund FWF (SFB LIPOTOX F3007 and F3012, DK-MCD W1226, as well as grants P29203, P29262, P27893, P31727) and the Austrian Federal Ministry of Education, Science and Research, as well as the University of Graz for grants "Unkonventionelle Forschung-InterFast and Fast4Health," as well as "flysleep" (BMWFW-80.109/0001-WF/V/3b/2015). We acknowledge the support of the Field of Excellence BioHealth, of NAWI Graz and the BioTechMed-Graz flagship project "EPIAge." B.R. acknowledges support by the European Union and is co-financed by the European Social Fund (grant agreement no. EFOP-3.6.2- 16-2017-00012; project title: Development of a product chain model for functional, healthy and safe foods from farm to fork based on a thematic research network). B.R. is also supported by the János Bolyai Research Fellowship from the Hungarian Academy of Sciences and by the ÚNKP-18-4 New National Excellence Program of the Ministry of Human Capacities. B.R. and P.S. were also supported by the National Research Development and Innovation Office (grant no. NKFIH-KKP-126998). L.S. and G.K. acknowledge funding by Leducq Foundation (TNE15004) and L.S. by Cariplo Foundation (7185). K.I. is supported by JSPS Program for Advancing Strategic International Networks to Accelerate the Circulation of Talented Researchers (grant no. S2603); "Japan Foundation for Pediatric Research," JSPS KAKENHI (grant no. JP19K08041); the Naito Foundation; and the Ichiro Kanehara Foundation for the Promotion of Medical Science & Medical Care. S. Sedej is supported by the Austrian Science Fund FWF through the grant I3301. S. Sedej and G.K. are supported by the European Research Area Network on Cardiovascular Diseases (ERA-CVD, MINOTAUR). The Bruneck study was funded by the "Pustertaler Verein zur Prävention von Herz- und Hirngefäßerkrankungen," the "Gesundheitsbezirk Bruneck," and the "Sanitätsbetrieb Südtirol," Province of Bolzano, Italy. R.P., H.T., and S.K. were supported by the excellence initiative (Competence Centers for Excellent Technologies [COMET]) of the Austrian Research Promotion Agency FFG: "Research Center of Excellence in Vascular Ageing" (K-Project No. 843536 and K-Centre 868624) funded by the Austrian Ministry for Transport, Innovation and Technology, the Austrian Ministry for Digital and Economic Affairs, and the federal states Tyrol (via Standortagentur), Salzburg, and Vienna (via Vienna Business Agency). M.Ü. was supported by the project LOGOS-TBI (Young Independent Researcher Groups, ZK-17), which is funded by the Austrian Science Fund FWF, and by the project CAMed (COMET K-Project 871132), which is funded by the Federal Ministry Republic of Austria Climate Action, Environment, Energy, Mobility, Innovation and Technology (BMK), the Federal Ministry Republic of Austria Digital and Economic Affairs (BMDW), and the Styrian Business Promotion Agency (SFG). T.M. was supported by the Austrian Science Fund (FWF) grants P28854, I3792, and DK-MCD W1226 and the Austrian Research Promotion Agency (FFG) grants 864690 and 870454; the Integrative Metabolism Research Center Graz; Austrian Infrastructure Program 2016/2017; the Styrian Government (Zukunftsfonds); and BioTechMed-Graz (Flagship project DYNIMO). We are thankful to Alexander J. Whitworth (University of Cambridge, Medical Research Council Mitochondrial Biology Unit) for *park25* mutants and to Gabor Juhasz (Eötvös Loránd University, Department of Anatomy, Cell and Developmental Biology) for *Atg7* mutants.

AUTHOR CONTRIBUTIONS

T.E., S.K., and F.M. designed and supervised the study; S. Schroeder, S.J.H. A.Z., R.P., D.C.-G., T.E., S.K., and F.M. wrote the manuscript and visualized the data. T.E., S. Schroeder, S.J.H., A.Z., C.D., T.P., G.M.M., V.P., M.B., M.M., V.G., S.R., J.T., K.I., G. Richter, A.F., M.Ü., M.P., P.R., R.M., M.A., R.C.T., T.M., F.S., C.M., J.D., B.R., and F.M. performed experiments and analyzed and discussed the data; R.P., J.W., B.M., H.N., I.P., G. Rungger, H.T., M.D., J.M., and S.K. performed epidemiological analyses and analyzed and discussed the data; U.S., P.S., T.R.P., P.H., G.K., L.S., S. Sedej, and S.J.S. gave conceptual advice.

DECLARATION OF INTERESTS

F.M., S.J.S., and D.C.-G. have equity interests in The Longevity Labs (TLL), a company founded in 2016 that develops natural food extracts. T.E. has equity interests in and conducts paid consultancies for TLL. G.K. holds research contracts with Bayer Healthcare, Genentech, GlaxoSmithKline, Institut Mérieux, Kaleido Biosciences, Lytix Biopharma, NuCana, Oncolinx, PharmaMar, Samsara Therapeutics, SOTIO, and Tioma Therapeutics. G.K. is on the Board of Directors of the Bristol Myers Squibb Foundation France. G.K. is a scientific cofounder of everImmune, a biotech company that develops immunostimulatory bacteria, and Therafast Bio. F.M. and T.E. are inventors on a pending patent application related to this work.

Received: June 3, 2019
Revised: February 8, 2021
Accepted: March 22, 2021
Published: April 13, 2021

REFERENCES

Ainsworth, B.E., Haskell, W.L., Whitt, M.C., Irwin, M.L., Swartz, A.M., Strath, S.J., O'Brien, W.L., Bassett, D.R., Jr., Schmitz, K.H., Emplaincourt, P.O., et al. (2000). Compendium of physical activities: an update of activity codes and MET intensities. Med. Sci. Sports Exerc. *32* (*9 Suppl*), S498–S504.

Atkinson, F.S., Foster-Powell, K., and Brand-Miller, J.C. (2008). International tables of glycemic index and glycemic load values: 2008. Diabetes Care *31*, 2281–2283.

Baecke, J.A., Burema, J., and Frijters, J.E. (1982). A short questionnaire for the measurement of habitual physical activity in epidemiological studies. Am. J. Clin. Nutr. *36*, 936–942.

Balschun, D., Wolfer, D.P., Gass, P., Mantamadiotis, T., Welzl, H., Schütz, G., Frey, J.U., and Lipp, H.-P. (2003). Does cAMP response element-binding protein have a pivotal role in hippocampal synaptic plasticity and hippocampus-dependent memory? J. Neurosci. *23*, 6304–6314.

Bass, T.M., Grandison, R.C., Wong, R., Martinez, P., Partridge, L., and Piper, M.D.W. (2007). Optimization of dietary restriction protocols in Drosophila. J. Gerontol. A Biol. Sci. Med. Sci. *62*, 1071–1081.

Bhukel, A., Beuschel, C.B., Maglione, M., Lehmann, M., Juhász, G., Madeo, F., and Sigrist, S.J. (2019). Autophagy within the mushroom body protects from synapse aging in a non-cell autonomous manner. Nat. Commun. *10*, 1318.

Bonora, E., Kiechl, S., Willeit, J., Oberhollenzer, F., Egger, G., Meigs, J.B., Bonadonna, R.C., and Muggeo, M.; Bruneck study (2004). Population-based incidence rates and risk factors for type 2 diabetes in white individuals: the Bruneck study. Diabetes *53*, 1782–1789.

Brand-Miller, J.C., Stockmann, K., Atkinson, F., Petocz, P., and Denyer, G. (2009). Glycemic index, postprandial glycemia, and the shape of the curve in healthy subjects: analysis of a database of more than 1,000 foods. Am. J. Clin. Nutr. *89*, 97–105.

Büttner, S., Broeskamp, F., Sommer, C., Markaki, M., Habernig, L., Alavian-Ghavanini, A., Carmona-Gutierrez, D., Eisenberg, T., Michael, E., Kroemer, G., et al. (2014). Spermidine protects against α-synuclein neurotoxicity. Cell Cycle *13*, 3903–3908.

Chong, J., Wishart, D.S., and Xia, J. (2019). Using MetaboAnalyst 4.0 for Comprehensive and Integrative Metabolomics Data Analysis. Curr. Protoc. Bioinformatics *68*, e86.

Chrisam, M., Pirozzi, M., Castagnaro, S., Blaauw, B., Polishchuck, R., Cecconi, F., Grumati, P., and Bonaldo, P. (2015). Reactivation of autophagy by spermidine ameliorates the myopathic defects of collagen VI-null mice. Autophagy *11*, 2142–2152.

Cornelissen, T., Vilain, S., Vints, K., Gounko, N., Verstreken, P., and Vandenberghe, W. (2018). Deficiency of parkin and PINK1 impairs age-dependent mitophagy in *Drosophila*. eLife *7*, e35878.

Cox, J., and Mann, M. (2008). MaxQuant enables high peptide identification rates, individualized p.p.b.-range mass accuracies and proteome-wide protein quantification. Nat. Biotechnol. *26*, 1367–1372.

De Risi, M., Torromino, G., Tufano, M., Moriceau, S., Pignataro, A., Rivagorda, M., Carrano, N., Middei, S., Settembre, C., Ammassari-Teule, M., et al. (2020). Mechanisms by which autophagy regulates memory capacity in ageing. Aging Cell *19*, e13189.

Eisenberg, T., Knauer, H., Schauer, A., Büttner, S., Ruckenstuhl, C., Carmona-Gutierrez, D., Ring, J., Schroeder, S., Magnes, C., Antonacci, L., et al. (2009). Induction of autophagy by spermidine promotes longevity. Nat. Cell Biol. *11*, 1305–1314.

Eisenberg, T., Abdellatif, M., Schroeder, S., Primessnig, U., Stekovic, S., Pendl, T., Harger, A., Schipke, J., Zimmermann, A., Schmidt, A., et al. (2016). Cardioprotection and lifespan extension by the natural polyamine spermidine. Nat. Med. *22*, 1428–1438.

FAO/WHO/UNU Expert Consultation (2005). Human energy requirements: report of a joint FAO/ WHO/UNU Expert Consultation. Food Nutr. Bull. *26*, 166.

Farzi, A., Reichmann, F., Meinitzer, A., Mayerhofer, R., Jain, P., Hassan, A.M., Fröhlich, E.E., Wagner, K., Painsipp, E., Rinner, B., and Holzer, P. (2015). Synergistic effects of NOD1 or NOD2 and TLR4 activation on mouse sickness behavior in relation to immune and brain activity markers. Brain Behav. Immun. *44*, 106–120.

Folstein, M.F., Folstein, S.E., and McHugh, P.R. (1975). "Mini-mental state". A practical method for grading the cognitive state of patients for the clinician. J. Psychiatr. Res. *12*, 189–198.

Gebhardt, S.E., Lemar, L.E., Pehrsson, P.R., Exler, J., Haytowitz, D.B., Showell, B.A., Nickle, M.S., Thomas, R.G., Patterson, K.K., Bhagwat, S.A., et al. 2010. USDA national nutrient database for standard reference, release 23. Available: http://www.ars.usda.gov/nutrientdata

Glatigny, M., Moriceau, S., Rivagorda, M., Ramos-Brossier, M., Nascimbeni, A.C., Lante, F., Shanley, M.R., Boudarene, N., Rousseaud, A., Friedman, A.K., et al. (2019). Autophagy Is Required for Memory Formation and Reverses Age-Related Memory Decline. Curr. Biol *29*, 435–448.e8.

Gnaiger, E., Kuznetsov, A.V., Schneeberger, S., Seiler, R., Brandacher, G., Steurer, W., and Margreiter, R. (2000). Mitochondria in the cold. In Life in the Cold, G. Heldmaier and M. Klingenspor, eds. (Springer), pp. 431–442.

Greene, J.C., Whitworth, A.J., Kuo, I., Andrews, L.A., Feany, M.B., and Pallanck, L.J. (2003). Mitochondrial pathology and apoptotic muscle degeneration in Drosophila parkin mutants. Proc. Natl. Acad. Sci. USA *100*, 4078–4083.

Grimm, A., and Eckert, A. (2017). Brain aging and neurodegeneration: from a mitochondrial point of view. J. Neurochem. *143*, 418–431.

Guerra, G.P., Rubin, M.A., and Mello, C.F. (2016). Modulation of learning and memory by natural polyamines. Pharmacol. Res. *112*, 99–118.

Gupta, V.K., Scheunemann, L., Eisenberg, T., Mertel, S., Bhukel, A., Koemans, T.S., Kramer, J.M., Liu, K.S.Y., Schroeder, S., Stunnenberg, H.G., et al. (2013). Restoring polyamines protects from age-induced memory impairment in an autophagy-dependent manner. Nat. Neurosci. *16*, 1453–1460.

Gupta, V.K., Pech, U., Bhukel, A., Fulterer, A., Ender, A., Mauermann, S.F., Andlauer, T.F.M., Antwi-Adjei, E., Beuschel, C., Thriene, K., et al. (2016). Spermidine Suppresses Age-Associated Memory Impairment by Preventing Adverse Increase of Presynaptic Active Zone Size and Release. PLoS Biol. *14*, e1002563.

Guze, S.B. (1995). Diagnostic and Statistical Manual of Mental Disorders, 4th ed. (DSM-IV). Am. J. Psychiatry *152*, 1228.

Haddadi, M., Jahromi, S.R., Sagar, B.K.C., Patil, R.K., Shivanandappa, T., and Ramesh, S.R. (2014). Brain aging, memory impairment and oxidative stress: a study in Drosophila melanogaster. Behav. Brain Res. *259*, 60–69.

Hara, T., Nakamura, K., Matsui, M., Yamamoto, A., Nakahara, Y., Suzuki-Migishima, R., Yokoyama, M., Mishima, K., Saito, I., Okano, H., and Mizushima, N. (2006). Suppression of basal autophagy in neural cells causes neurodegenerative disease in mice. Nature *441*, 885–889.

Hill, A.B. (1965). The environment and disease: association or causation? Proc. R. Soc. Med. *58*, 295–300.

Jin, S.M., and Youle, R.J. (2012). PINK1- and Parkin-mediated mitophagy at a glance. J. Cell Sci. *125*, 795–799.

Jobim, P.F.C., Pedroso, T.R., Christoff, R.R., Werenicz, A., Maurmann, N., Reolon, G.K., and Roesler, R. (2012). Inhibition of mTOR by rapamycin in the amygdala or hippocampus impairs formation and reconsolidation of inhibitory avoidance memory. Neurobiol. Learn. Mem. *97*, 105–112.

Juhász, G., Erdi, B., Sass, M., and Neufeld, T.P. (2007). Atg7-dependent autophagy promotes neuronal health, stress tolerance, and longevity but is dispensable for metamorphosis in Drosophila. Genes Dev. *21*, 3061–3066.

Kann, O., and Kovács, R. (2007). Mitochondria and neuronal activity. Am. J. Physiol. Cell Physiol. *292*, C641–C657.

Kennard, J. (2011). Age sensitivity of behavioral tests and brain substrates of normal aging in mice. Front. Aging Neurosci. *3*, 9.

Kiechl, S., and Willeit, J. (2019). In a Nutshell: Findings from the Bruneck Study. Gerontology *65*, 9–19.

Kiechl, S., Wittmann, J., Giaccari, A., Knoflach, M., Willeit, P., Bozec, A., Moschen, A.R., Muscogiuri, G., Sorice, G.P., Kireva, T., et al. (2013). Blockade of receptor activator of nuclear factor-κB (RANKL) signaling improves hepatic insulin resistance and prevents development of diabetes mellitus. Nat. Med. *19*, 358–363.

Kiechl, S., Pechlaner, R., Willeit, P., Notdurfter, M., Paulweber, B., Willeit, K., Werner, P., Ruckenstuhl, C., Iglseder, B., Weger, S., et al. (2018). Higher spermidine intake is linked to lower mortality: a prospective population-based study. Am. J. Clin. Nutr. *108*, 371–380.

Komatsu, M., Waguri, S., Chiba, T., Murata, S., Iwata, J., Tanida, I., Ueno, T., Koike, M., Uchiyama, Y., Kominami, E., and Tanaka, K. (2006). Loss of autophagy in the central nervous system causes neurodegeneration in mice. Nature *441*, 880–884.

Liu, S., Willett, W.C., Stampfer, M.J., Hu, F.B., Franz, M., Sampson, L., Hennekens, C.H., and Manson, J.E. (2000). A prospective study of dietary glycemic load, carbohydrate intake, and risk of coronary heart disease in US women. Am. J. Clin. Nutr. *71*, 1455–1461.

Maglione, M., Kochlamazashvili, G., Eisenberg, T., Rácz, B., Michael, E., Toppe, D., Stumpf, A., Wirth, A., Zeug, A., Müller, F.E., et al. (2019). Spermidine protects from age-related synaptic alterations at hippocampal mossy fiber-CA3 synapses. Sci. Rep. *9*, 19616.

Magnes, C., Fauland, A., Gander, E., Narath, S., Ratzer, M., Eisenberg, T., Madeo, F., Pieber, T., and Sinner, F. (2014). Polyamines in biological samples: rapid and robust quantification by solid-phase extraction online-coupled to liquid chromatography-tandem mass spectrometry. J. Chromatogr. A *1331*, 44–51.

Mapstone, M., Cheema, A.K., Fiandaca, M.S., Zhong, X., Mhyre, T.R., MacArthur, L.H., Hall, W.J., Fisher, S.G., Peterson, D.R., Haley, J.M., et al. (2014). Plasma phospholipids identify antecedent memory impairment in older adults. Nat. Med. *20*, 415–418.

Masuda, A., Kobayashi, Y., Kogo, N., Saito, T., Saido, T.C., and Itohara, S. (2016). Cognitive deficits in single App knock-in mouse models. Neurobiol. Learn. Mem. *135*, 73–82.

McCullough, M.L., Feskanich, D., Stampfer, M.J., Giovannucci, E.L., Rimm, E.B., Hu, F.B., Spiegelman, D., Hunter, D.J., Colditz, G.A., and Willett, W.C. (2002). Diet quality and major chronic disease risk in men and women: moving toward improved dietary guidance. Am. J. Clin. Nutr. *76*, 1261–1271.

Mechan, A.O., Wyss, A., Rieger, H., and Mohajeri, M.H. (2009). A comparison of learning and memory characteristics of young and middle-aged wild-type mice in the IntelliCage. J. Neurosci. Methods *180*, 43–51.

Mifflin, M.D., St Jeor, S.T., Hill, L.A., Scott, B.J., Daugherty, S.A., and Koh, Y.O. (1990). A new predictive equation for resting energy expenditure in healthy individuals. Am. J. Clin. Nutr. *51*, 241–247.

Mikolajczak, P., Okulicz-Kozaryn, I., Polanska, A., Szczawinska, K., and Bobkiewicz-Kozlowska, T. (2002). Effect of multiple ifenprodil or spermidine treatment on social recognition in rats. J. Basic Clin. Physiol. Pharmacol. *13*, 61–67.

Morris, J.C., Heyman, A., Mohs, R.C., Hughes, J.P., van Belle, G., Fillenbaum, G., Mellits, E.D., and Clark, C. (1989). The Consortium to Establish a Registry for Alzheimer's Disease (CERAD). Part I. Clinical and neuropsychological assessment of Alzheimer's disease. Neurology *39*, 1159–1165.

Morselli, E., Mariño, G., Bennetzen, M.V., Eisenberg, T., Megalou, E., Schroeder, S., Cabrera, S., Bénit, P., Rustin, P., Criollo, A., et al. (2011). Spermidine and resveratrol induce autophagy by distinct pathways converging on the acetylproteome. J. Cell Biol. *192*, 615–629.

Murman, D.L. (2015). The Impact of Age on Cognition. Semin. Hear. *36*, 111–121.

Navarro, A., and Boveris, A. (2007). The mitochondrial energy transduction system and the aging process. Am. J. Physiol. Cell Physiol. *292*, C670–C686.

Ott, C., König, J., Höhn, A., Jung, T., and Grune, T. (2016). Macroautophagy is impaired in old murine brain tissue as well as in senescent human fibroblasts. Redox Biol. *10*, 266–273.

Puleston, D.J., Buck, M.D., Klein Geltink, R.I., Kyle, R.L., Caputa, G., O'Sullivan, D., Cameron, A.M., Castoldi, A., Musa, Y., Kabat, A.M., et al. (2019). Polyamines and eIF5A Hypusination Modulate Mitochondrial Respiration and Macrophage Activation. Cell Metab. *30*, 352–363.e8.

Qi, Y., Qiu, Q., Gu, X., Tian, Y., and Zhang, Y. (2016). ATM mediates spermidine-induced mitophagy via PINK1 and Parkin regulation in human fibroblasts. Sci. Rep. *6*, 24700.

Robinson, L., and Riedel, G. (2014). Comparison of automated home-cage monitoring systems: emphasis on feeding behaviour, activity and spatial learning following pharmacological interventions. J. Neurosci. Methods *234*, 13–25.

Roth, M., Tym, E., Mountjoy, C.Q., Huppert, F.A., Hendrie, H., Verma, S., and Goddard, R. (1986). CAMDEX. A standardised instrument for the diagnosis of mental disorder in the elderly with special reference to the early detection of dementia. Br. J. Psychiatry *149*, 698–709.

Schwarz, C., Stekovic, S., Wirth, M., Benson, G., Royer, P., Sigrist, S.J., Pieber, T., Dammbrueck, C., Magnes, C., Eisenberg, T., et al. (2018). Safety and tolerability of spermidine supplementation in mice and older adults with subjective cognitive decline. Aging (Albany NY) *10*, 19–33.

Schwarz, C., Horn, N., Benson, G., Wrachtrup Calzado, I., Wurdack, K., Pechlaner, R., Grittner, U., Wirth, M., and Flöel, A. (2020). Spermidine intake is associated with cortical thickness and hippocampal volume in older adults. Neuroimage *221*, 117132.

Shetty, P.K., Galeffi, F., and Turner, D.A. (2011). Age-Induced Alterations in Hippocampal Function and Metabolism. Aging Dis. *2*, 196–218.

Shi, R., Guberman, M., and Kirshenbaum, L.A. (2018). Mitochondrial quality control: The role of mitophagy in aging. Trends Cardiovasc. Med. *28*, 246–260.

Shin, W.-W., Fong, W.-F., Pang, S.-F., and Wong, P.C.-L. (1985). Limited blood-brain barrier transport of polyamines. J. Neurochem. *44*, 1056–1059.

Srivastava, S. (2017). The Mitochondrial Basis of Aging and Age-Related Disorders. Genes (Basel) *8*, 398.

Stegemann, C., Pechlaner, R., Willeit, P., Langley, S.R., Mangino, M., Mayr, U., Menni, C., Moayyeri, A., Santer, P., Rungger, G., et al. (2014). Lipidomics profiling and risk of cardiovascular disease in the prospective population-based Bruneck study. Circulation *129*, 1821–1831.

Sun, N., Youle, R.J., and Finkel, T. (2016). The Mitochondrial Basis of Aging. Mol. Cell *61*, 654–666.

Todorova, V., and Blokland, A. (2017). Mitochondria and Synaptic Plasticity in the Mature and Aging Nervous System. Curr. Neuropharmacol. *15*, 166–173.

Tölle, R.C., Gaggioli, C., and Dengjel, J. (2018). Three-Dimensional Cell Culture Conditions Affect the Proteome of Cancer-Associated Fibroblasts. J. Proteome Res. *17*, 2780–2789.

Tsoi, K.K.F., Chan, J.Y.C., Hirai, H.W., Wong, S.Y.S., and Kwok, T.C.Y. (2015). Cognitive Tests to Detect Dementia: A Systematic Review and Meta-analysis. JAMA Intern. Med. *175*, 1450–1458.

Tully, T., and Quinn, W.G. (1985). Classical conditioning and retention in normal and mutant Drosophila melanogaster. J. Comp. Physiol. A Neuroethol. Sens. Neural Behav. Physiol. *157*, 263–277.

Wang, I.-F., Guo, B.-S., Liu, Y.-C., Wu, C.-C., Yang, C.-H., Tsai, K.-J., and Shen, C.-K.J. (2012). Autophagy activators rescue and alleviate pathogenesis of a mouse model with proteinopathies of the TAR DNA-binding protein 43. Proc. Natl. Acad. Sci. USA *109*, 15024–15029.

Welsh, K.A., Butters, N., Mohs, R.C., Beekly, D., Edland, S., Fillenbaum, G., and Heyman, A. (1994). The Consortium to Establish a Registry for Alzheimer's Disease (CERAD). Part V. A normative study of the neuropsychological battery. Neurology *44*, 609–614.

Willeit, P., Kiechl, S., Kronenberg, F., Witztum, J.L., Santer, P., Mayr, M., Xu, Q., Mayr, A., Willeit, J., and Tsimikas, S. (2014). Discrimination and net reclassification of cardiovascular risk with lipoprotein(a): prospective 15-year outcomes in the Bruneck Study. J. Am. Coll. Cardiol. *64*, 851–860.

Willett, W., and Stampfer, M.J. (1986). Total energy intake: implications for epidemiologic analyses. Am. J. Epidemiol. *124*, 17–27.

Willett, W.C., Sampson, L., Stampfer, M.J., Rosner, B., Bain, C., Witschi, J., Hennekens, C.H., and Speizer, F.E. (1985). Reproducibility and validity of a semiquantitative food frequency questionnaire. Am. J. Epidemiol. *122*, 51–65.

Wirth, M., Benson, G., Schwarz, C., Köbe, T., Grittner, U., Schmitz, D., Sigrist, S.J., Bohlken, J., Stekovic, S., Madeo, F., and Flöel, A. (2018). The effect of spermidine on memory performance in older adults at risk for dementia: A randomized controlled trial. Cortex *109*, 181–188.

Xu, T.-T., Li, H., Dai, Z., Lau, G.K., Li, B.-Y., Zhu, W.-L., Liu, X.-Q., Liu, H.-F., Cai, W.-W., Huang, S.-Q., et al. (2020). Spermidine and spermine delay brain aging by inducing autophagy in SAMP8 mice. Aging (Albany NY) *12*, 6401–6414.

Yang, F., Chu, X., Yin, M., Liu, X., Yuan, H., Niu, Y., and Fu, L. (2014). mTOR and autophagy in normal brain aging and caloric restriction ameliorating age-related cognition deficits. Behav. Brain Res. *264*, 82–90.

Yang, X., Zhang, M., Dai, Y., Sun, Y., Aman, Y., Xu, Y., Yu, P., Zheng, Y., Yang, J., and Zhu, X. (2020). Spermidine inhibits neurodegeneration and delays aging via the PINK1-PDR1-dependent mitophagy pathway in *C. elegans*. Aging (Albany NY) *12*, 16852–16866.

Yorimitsu, T., and Klionsky, D.J. (2005). Autophagy: molecular machinery for self-eating. Cell Death Differ. *12* (*Suppl 2*), 1542–1552.

Zhang, J., Culp, M.L., Craver, J.G., and Darley-Usmar, V. (2018). Mitochondrial function and autophagy: integrating proteotoxic, redox, and metabolic stress in Parkinson's disease. J. Neurochem. *144*, 691–709.

Zhang, H., Alsaleh, G., Feltham, J., Sun, Y., Napolitano, G., Riffelmacher, T., Charles, P., Frau, L., Hublitz, P., Yu, Z., et al. (2019). Polyamines Control eIF5A Hypusination, TFEB Translation, and Autophagy to Reverse B Cell Senescence. Mol. Cell *76*, 110–125.e9.

STAR★METHODS

KEY RESOURCES TABLE

REAGENT or RESOURCE	SOURCE	IDENTIFIER
Antibodies		
GAPDH	CST	Cat#2118; RRID:AB_561053
rabbit-IgG-HRP	CST	Cat#7074; RRID: AB_2099233
PKA	CST	Cat#4782; RRID:AB_2170170
Phospho-PKA	CST	Cat#4781; RRID:AB_2300165
CREB	Abcam	Cat#ab32515; RRID:AB_2292301
Phospho-CREB	Abcam	Cat#ab32096; RRID:AB_731734
CaMKII alpha	Abcam	Cat#ab103840; RRID:AB_10900968
Phospho-CaMKII alpha	Abcam	Cat#ab5683; RRID:AB_305050
eIF5A	Beckton-Dickinson	Cat#BD611976; RRID:AB_399397
Hypusine	Merck	Cat#ABS1064-I; RRID:AB_2631138
TFEB	Bethyl Labs	Cat#A303-673A; RRID:AB_11204751
mouse-IgG-HRP	Sigma-Aldrich	Cat#A9044; RRID:AB_258431
Chemicals, peptides, and recombinant proteins		
Spermidine free base	Sigma-Aldrich	Cat#85558
Standard chow for mice	Ssniff	Cat#V1536
Stable isotope labeled SPD (8-fold deuterated, SPD-(butyl-d8) trihydrochloride	Sigma-Aldrich	Cat#709891
3-octanol	Sigma-Aldrich	Cat#218405
4-methylcyclohexanol (mixture of cis and trans)	Sigma-Aldrich	Cat#153095
Paraffin oil	Sigma-Aldrich	Cat#18512
BSA (fatty acid free)	Sigma-Aldrich	Cat#A6003
Lactobionic acid	Sigma-Aldrich	Cat#153516
Malic acid	Sigma-Aldrich	Cat#M1125
Carbonyl cyanide m-chlorophenyl hydrazone (CCCP)	Sigma-Aldrich	Cat#C2759
Glutamate	Sigma-Aldrich	Cat#G1626
Pyruvate	Sigma-Aldrich	Cat#P2256
ADP	Sigma-Aldrich	Cat#A5285
Cytochrome *c*	Sigma-Aldrich	Cat#C7752
Succinate	Sigma-Aldrich	Cat#S2378
Rotenone	Sigma-Aldrich	Cat#R8875
Antimycin A	Sigma-Aldrich	Cat#A8674
PhosSTOP	Roche	Cat#04906837001
HALT Protease Inhibitor Cocktail	Thermo Scientific	Cat#78439
Protein Assay Reagent	BioRad	Cat#500-0006
NuPAGE Novex Bis-Tris Gels 12%	Invitrogen	Cat#NP0343
ECL	BioRad	Cat#170-5061
100 μm cell strainer	Corning	Cat#431752
4–12% Bis-Tris gradient gels	Invitrogen	Cat#NP0321
Trypsin	Promega	Cat#V5280
Sodium phosphate, dibasic (Na_2HPO_4)	VWR International	Cat#28026.292
Sodium hydroxide	VWR International	Cat# M137-1KG
Hypochlorous acid (32% m/v)	VWR International	Cat# 20254.310

(*Continued on next page*)

Continued

REAGENT or RESOURCE	SOURCE	IDENTIFIER
Sodium azide (NaN_3)	VWR International	Cat# 0639-250G
3(trimethylsilyl) propionic acid-2,2,3,3-d_4 sodium salt	Alfa Aesar	Cat#A14489.06
Deuterium oxide (D_2O)	Cambridge Isotopes laboratories	Cat#DLM-4-99.8-1000
Drosophila vials small (28mm diameter)	K-TK e.K.	Cat#40300
Drosophila vials large (48mm diameter)	K-TK e.K.	Cat#41171
Baker's yeast	Lesaffre	Cat#AR2502
p-Hydroxybenzoic acid methyl ester (Nipagin)	Sigma-Aldrich	Cat#W271004
Propionic acid	Sigma-Aldrich	Cat#P5561
Cornmeal	Schälmühle Nestelberger	Cat#SN-Maismehl
Soymeal	Schälmühle Nestelberger	Cat#SN-Sojamehl
Sugar syrup	Bioinsel Rosenberger	Cat#156667
Ketamidor 100mg/dl (Ketamine)	Richter Pharma	Authorisation number 8-01141
Rompun 20mg/ml (Xylazin)	Bayer HealthCare	Authorsiation number 8-14840
Acetonitril chromasolv for HPLC, gradient grade	Sigma-Aldrich	Cat#34851
Acetic acid puriss., 99.8-100.5% /	Sigma-Aldrich	Cat#27225
Deposited data		
MS-based proteomics data	PRIDE DB	PXD022614
Experimental models: Organisms/strains		
C57BL/6J:Rj wild-type male mice	Janvier Labs, France	Cat#SC-C57J-M
C57BL/6JRccHsd wild-type female mice	Envigo, Italy	Cat#4367F
Drosophila, w[1118]	Stephan Sigrist, Gupta et al., 2013 (https://doi.org/10.1038/nn.3512)	N/A
Drosophila, P{w[+m] = Appl-GAL4.G1a}1, y[1] w[*]* (neuronal GAL4 driver)	Bloomington Drosophila Stock Center	Cat#32040
Drosophila, y, w[1118]; P{KK101205}VIE-260B (UAS-IR^{Pink1} flies)	Vienna Drosophila Resource Center	Cat#109614
Drosophila, y, w[1118]; P{attP,y[+],w[3'} (landing site control for UAS-IR^{Pink1} flies)	Vienna Drosophila Resource Center	Cat#60100
Drosophila, w[*]; Atg7[d14]/CyO, P{3xP3-EGFP}2	Gabor Juhasz, Juhasz et al., 2007 (https://doi.org/10.1101/gad.1600707)	N/A
Drosophila, w[*]; Atg7[d30]/CyO, P{3xP3-EGFP}2	Gabor Juhasz, Juhasz et al., 2007 (https://doi.org/10.1101/gad.1600707)	N/A
Drosophila, w[*]; Atg7[d77]/CyO, P{3xP3-EGFP}2	Gabor Juhasz, Juhasz et al., 2007 (https://doi.org/10.1101/gad.1600707)	N/A
Drosophila, w[*]; Park[25]/TM6B-GFP (*$Park^{25}$* mutant flies)	Alexander J Whitworth, Greene et al., 2013 (https://doi.org/10.1073/pnas.0737556100)	N/A
Software and algorithms		
MaxQuant, 1.4.1.2	Cox et al., 2008 (https://doi.org/10.1038/nbt.1511)	https://www.maxquant.org/
Metaboanalyst 4.0	https://doi.org/10.1002/cpbi.86	https://www.metaboanalyst.ca/
Topspin version 4.0.2	Bruker Biospin	https://www.bruker.com/en/products-and-solutions/mr/nmr-software.html
MestReNova 11.0	Mestrelab	https://mestrelab.com/

(*Continued on next page*)

Continued

REAGENT or RESOURCE	SOURCE	IDENTIFIER
ImageLab	Bio-Rad laboratories	http://www.bio-rad.com/en-us/product/image-lab-software?ID=KRE6P5E8Z
Prism 9.0.0	GraphPad	https://www.graphpad.com/
OriginPro 8	OriginLab Corporation	https://www.originlab.com/
R 3.2.2 (R Foundation for Statistical Computing, Vienna, Austria)	R Core Team (2012). R: A language and environment for statistical computing. R Foundation for Statistical Computing, Vienna, Austria. ISBN 3-900051-07-0	https://www.r-project.org/
IBM SPSS Statistics Version 22	IBM Corporation New Orchard Road Armonk, NY 10504	https://www.ibm.com/us-en/?ar=1
VideoMot2 video tracking system (incl. a 12V black & white CCD Camera, Eneo VK1316S)	TSE Systems GmbH, Germany	https://www.tse-systems.com/service/videomot2/
Xcalibur	Thermo Fisher Scientific	Vers. 4.027.21
Other		
LTQ Orbitrap XL	Thermo Fisher Scientific	https://planetorbitrap.com/
QExactive	Thermo Fisher Scientific	https://planetorbitrap.com/
EasyLC 1000	Thermo Fisher Scientific	https://www.thermofisher.com/order/catalog/product/LC120#/LC120
Reprosil–Pur 120 ODS–3, 1.9 μm	Dr. Maisch	https://dr-maisch.com/dr-maisch-phases/reprosil-pur/reprosil-pur-120-ods-3
Tecniplast Type 2L Mouse cage	Tecniplast	https://www.tecniplast.it/
IntelliCage	TSE Systems, Bad Homburg, Germany	https://www.tse-systems.com/product-details/intellicage/
AVANCE Neo Bruker Ultrashield 600 MHz spectrometer	Bruker Biospin	https://www.bruker.com/en/products-and-solutions/mr/nmr.html
ChemiDoc imaging system	BioRad	https://www.bio-rad.com/en-us/category/chemidoc-imaging-systems?ID=NINJ0Z15
Oxygraph-2k high-resolution respirometer	Oroboros Instruments, Austria	https://www.oroboros.at/index.php/o2k-products/
Morris Water Maze	TSE Systems GmbH, Germany	https://www.tse-systems.com/water-maze/
Tully Drosophila T-maze	CON-Elektronik, Greussenheim, Germany	http://www.con-elektronik.de/
CERAD 1.0	Welsh et al., 1994 Morris et al., 1989	https://www.memoryclinic.ch/de/main-navigation/neuropsychologen/cerad-plus/auswertungprogramme/cerad-plus-10-excel/
Strata-X 33 μm Polymeric Reversed Phase, 10 mg/well, 96 Well Plate	Phenomenex	Cat#8E-S100-ABG
Kinetex 2.6 μm C18 100A 50mm × 2.1mm	Phenomenex	Cat#00B-4462-AN
TSQ Quantum Ultra AM	Thermo Fisher Scientific	N/A
U3000 UHPLC	Thermo Fisher Scientific	N/A

RESOURCE AVAILABILITY

Lead contact

Further information and requests for resources and reagents should be directed to and will be fulfilled by the Lead Contact, Frank Madeo (frank.madeo@uni-graz.at).

Materials availability

This study did not generate new unique reagents.

Data and code availability

This study did not generate any unique code. The accession number for the MS proteomics data (Figure S1) reported in this paper is PRIDE: PXD022614 Data from the Bruneck Study are available in accordance and in consent with ethical permission for use in independent scientific research to researchers upon reasonable request. Data will be provided following review and approval of a research proposal (including a statistical analysis plan) and completion of a data sharing agreement between the governing legal entities. All other source data will be provided by the Lead Contact upon request.

EXPERIMENTAL MODEL AND SUBJECT DETAILS

Animal strains and housing

C57BL/6J:Rj wild-type male mice were purchased from Janvier Labs, France, C57BL/6JRccHsd wild-type female mice were purchased from Envigo, Italy. Supplementation of spermidine (SPD) was conducted late-in-life (starting at 18 months of age) as previously described (Eisenberg et al., 2016). Middle-aged (13-month old) mice were supplemented with SPD for 5 months, starting at the age of 8 months. Young animals were supplemented for 3 months, starting at the age of 2 months. Briefly, animals were housed in groups of two to four animals per cage under specific-pathogen-free (SPF) conditions in a 14h/10h light/dark cycle with *ad libitum* access to standard chow (Ssniff, cat. #V1536) and autoclaved tap water. Autoclaved nest material and one paper house per cage served as cage enrichment. All animal experiments were performed in accordance with national and European ethical regulation (Directive 2010/63/EU) and approved by the responsible institutional or government agencies (Bundesministerium für Wissenschaft, Forschung und Wirtschaft, BMWFW, Austria: BMWF-66.007/0011-II/3b/2013, BMWFW-66.007/0002-WF/V/3b/2015, BMWFW-66.007/0024-WF/V/3b/2015, BMWFW-66.007/0025-WF/V/3b/2016, BMWFW-66.007/0032-V/3b/2019).

Fly strains

For the assessment of respiratory competence, male and female w^{1118} flies were used. For Pink1-RNAi experiments, *Appl-GAL4* driver flies for neuronal Gal4 expression (BDSC #32040) and *UAS-IR*^{Pink1} flies (VDRC KK #109614) or isogenic controls (VDRC #60100) were used. $Atg7^{d14}$, $Atg7^{d30}$ and $Atg7^{d77}$ mutants were a kind gift of Gabor Juhasz (Eötvös Loránd University, Department of Anatomy, Cell and Developmental Biology) (Juhász et al., 2007). To control for heterozygosity of the affected loci *Sec6* and *CG5335* in these flies, $Atg7^{d14/d77}$ mutants (heterozygous for *Sec6* and *CG5335*, null mutant for *Atg7*) were compared to $Atg7^{d14/d30}$ mutants (heterozygous for *Sec6*, *CG5335* and *Atg7*). $Park^{25}$ mutants were a kind gift from Alexander J Whitworth (University of Cambridge, Medical Research Council Mitochondrial Biology Unit) (Greene et al., 2003). Wherever applicable, fly strains were isogenized for at least six generations before being compared to each other.

Human study subjects

The Bruneck Study is a prospective population-based cohort study enrolled in 1990 as an age- and sex-stratified random sample of the inhabitants of Bruneck (Italy) aged 40-79 and re-evaluations were scheduled every five years since (Eisenberg et al., 2016; Kiechl et al., 2013; Stegemann et al., 2014; Willeit et al., 2014)· The population is exclusively Caucasian and unique for its participation and in-person follow-up rates exceeding 90% (Eisenberg et al., 2016; Kiechl et al., 2013; Stegemann et al., 2014; Willeit et al., 2014). Baseline characteristics of the Bruneck Study cohort, including information on gender/sex are summarized in Table S3. For this analysis, we defined 1995 as the baseline because this was the year of the first detailed dietary assessment. The study protocol conformed to the Declaration of Helsinki and was approved by the local ethics committees (Bolzano and Verona). Participants gave their written informed consent.

METHOD DETAILS

Spermidine (SPD) supplementation of mice

SPD (3 or 6 mM final concentration, as indicated) was prepared from aqueous stock solutions (1 M, adjusted to pH of 7.2 - 7.4), and was administered *ad libitum* via autoclaved drinking water. Control animals received regular autoclaved drinking water. SPD supplemented drinking water was freshly prepared every 3-4 days and stability of SPD was confirmed by LC-MS analysis in separate water bottles prior to the experiments. For preparation of SPD stock solutions "spermidine free base" (Sigma-Aldrich #85558) was carefully titrated (slowly on ice to prevent the solution of heating up) to pH 7.2-7.4 using hydrochloric acid. The stock solution appeared clear

and colorless after pH adjustment. The pH adjusted stock solution was then sterile filtered and stored for up to 3 months at −80°C in single use aliquots.

Tissue preparation of mouse brains

Mouse brain tissue was dissected after euthanizing the animal by cervical dislocation under isoflurane anesthesia and either snap-frozen and stored in liquid nitrogen (e.g., before polyamine- or protein-extraction) or directly processed for high-resolution respirometry. For determination of d8-labeled SPD tissue levels mice were deeply anesthetized with ketamine (100 mg/kg body weight) and xylazine (5 mg/kg body weight) and perfused transcardially (see below).

Quantification of cerebral bioavailability of spermidine (SPD) by mass spectrometry (MS)

To assess cerebral bioavailability of dietary SPD, drinking water of 18-month-old aging mice was supplemented with 3 mM SPD containing 3%–5% (molar ratio) of stable isotope labeled SPD (8-fold deuterated, SPD-(butyl-d8) trihydrochloride, Sigma-Aldrich #709891) for 1, 4 and 8 weeks. The brain tissue from these animals were subsequently analyzed for presence of deuterated SPD and normalized to whole blood levels in order to assess its bioavailability from circulation: For tissue collection, brains were transcardially perfused with 0.9% saline for 2 min in order to remove blood from brain tissue and thus prevent contamination of brain tissue from polyamines in circulation. An aliquot of whole blood was taken by cardiac puncture prior to perfusion, transferred to appropriate EDTA-collection tube and stored at −80°C upon polyamine extraction. After perfusion, brains were quickly excised, separated into sub-regions on ice, and immediately snap frozen in liquid nitrogen. Polyamine extraction and quantification using high performance liquid chromatography coupled to mass spectrometry (LC-MS). Briefly, tissue polyamines were extracted from 25 μl whole blood or the total amount of brain sub-regions (~20 – 130 mg depending on the respective sub-region) using appropriate volumes of 5% trichloroacetic acid and derivatized using isobutyl chloroformate as previously described (Magnes et al., 2014) with following adaptations: polyamine derivatives were extracted by SPE (Strata-X, Polymeric Reversed Phase, 96-well plate). SPE was conditioned with 500 μl acetonitrile, equilibrated with 500 μl dest. water containing 0.2% acetic acid. Trichloroacetic acid extracts were loaded onto the SPE and after two washing steps with 500 μl 0.2% acetic acid samples were eluted with 250 μl 80% acetonitrile containing 0.2% acetic acid. Eluted SPE extracts were subjected to LC-MS (mobile phase: isocratic 80% acetontirle containing 0.2% acetic acid; flow rate 250 μl/min; HPLC column: Kinetex 2.6 μm C18 100 A 50 mm × 2.1 mm) MRM transitions chosen for SPD were mz 446.4 → 298.1 and 454.4 → 306.1 for d8-SPD. The presence of (dietary-supplied) d8-SPD was calculated using peak intensities of d8-SPD divided by that of unlabeled SPD (area ratios). Area ratios from the various brain sub-regions were normalized to the respective area ratios of whole blood and used as an estimate of cerebral bioavailability of SPD from circulation. Of note, at the 1-week feeding time point, one blood sample was lost due to technical problems and the mean of the two other samples was used for normalization of the respective brain samples.

Mass spectrometry-based proteomics of brain tissue

Samples were basically processed as described (Tölle et al., 2018). Briefly, whole tissue lysates were separated by SDS–PAGE using 4%–12% Bis-Tris gradient gels (Invitrogen). Gel lanes were cut into 10 slices, proteins therein were digested with trypsin (Promega), peptides were purified by STAGE tips and analyzed by LC-MS/MS.

MS analyses were conducted on an LTQ Orbitrap XL and on a QExactive Plus mass spectrometer, both coupled to EasyLCs 1000 (all Thermo Fisher Scientific). LC columns (75 μm inner diameter) were packed in-house with Reprosil–Pur 120 ODS–3 (Dr. Maisch). Samples were applied to the column with a gradient of A (0.5% acetic acid) and B (0.5% acetic acid in 80% acetonitrile) with increasing acetonitrile proportion for peptide separation. Samples were separated over 100 min by increasing the percentage of buffer B to 35%. The spray voltage was 2.3 kV with no sheath and auxiliary gas flow. Data were acquired in data-dependent mode and switched automatically between MS and MS/MS with a maximum of 1×10^6 ions in MS. The top five (top 10 for QExactive) most abundant peptides were isolated and fragmented with 35% collision energy (25% for the QExactive) and a target value of 5‘000. Parent ions with a charge state of z = 1 and unassigned charge states were excluded from fragmentation. The mass range for the LTQ Orbitrap was set to 350–2000 m/z with a resolution of 60‘000, for the QExactive Plus the mass range was 370-1750 m/z with a resolution of 70‘000.

Raw mass spectra data were searched with the MaxQuant software version 1.4.1.2 (Cox and Mann, 2008) using a UniProt mouse database from April 2016. The defined fixed modification was carbamidomethylation of cysteines, whereas methionine oxidations and protein amino-terminal acetylations were set as variable modifications. Three missed cleavages were allowed for enzymatic cleavage with trypsin/P. Quantitation was done by LFQ. FTMS MS/MS tolerance was set to 20 ppm, LTQ MS/MS tolerance to 0.5 Da. FDRs of 0.01 were applied for peptide and protein identification, the minimum peptide length was set to seven, and at least one peptide was unique. For quantification, a minimum ratio count of two was chosen. Identified proteins were re-quantified.

The proteomics data were filtered manually and proteins with more than two missing values in one of the groups were excluded. Remaining missing values were replaced by 1/5 of the minimum positive value of each protein. The data were log-transformed and auto-scaled (mean-centered and divided by the standard deviation of each variable) in Metaboanalyst 4.0 (Chong et al., 2019). Differences between 24-month-old (Aged) and 24-month-old SPD-fed animals (SPD) were detected by foldchange differences > 2 or < 0.5 between the two groups and statistical significance was assessed by raw p values < 0.05, due to the explorative nature of the experiment. Data visualization of this subset of proteins (FC > 2 or < 0.5 between Aged and SPD) was performed in Metaboanalyst

4.0 (Chong et al., 2019). The 4-month-old (Young) group was included as a reference group but had no influence on the selection of the proteins.

IntelliCage

The IntelliCage (TSE Systems, Bad Homburg, Germany) was placed in a polycarbonate cage (20.5 cm high; 58 cm × 40 cm top; 55 cm × 37.5 cm bottom), which accommodates up to 16 mice. Due to the advanced age of the mice used, only up to 12 animals from the same group were tested at the same time. Only animals that fully completed a respective task were used for data analysis. The groups were not mixed. The IntelliCage contains a freely accessible metal rack with standard chow food. The floor was covered with autoclaved standard bedding and provides 4 central shelter houses. Four triangular conditioning chambers (15 cm × 15 cm × 21 cm) are fitted in each corner of the cage and provide room for one mouse at once. Each chamber contains two drinking bottles (left and right side of the chamber), accessible via two round openings (13 mm diameter) with motorized doors. Each chamber contains 3 LED lights and a motorized valve for air puffs above the doors. Under mild isoflurane inhalation induced anesthesia (for max. 2 min), each mouse was injected subcutaneously in the dorso-cervical area with a RFID antenna one week prior to entering the cage, allowing the identification of each mouse while visiting any corner. During a visit to a corner, its duration and the number of individual nose-pokes at each door were recorded using IR-beam sensors. Furthermore, the number of licks at each bottle was monitored using lick-o-meters, including the duration of individual licks. Visual clues (items or symbols printed on paper) were placed at each side of the cage that allowed the animals to visually orientate.

We used two testing schemes in different cohorts, adapted from Mechan et al. (2009) and Masuda et al. (2016): The first protocol consisted of (i) a habituation phase (4 days) in which all doors were open and mice had free access to water, followed by a (ii) nose-poke learning phase (2 days) in which the doors were closed unless mice performed a nose-poke at the door (data not shown). Successfully opened doors were automatically closed after 5 s. We included a (iii) water-restriction phase in which water access was subsequently reduced over 4 days until access was only given two times a day for one hour (00-01 am and 05-06 am) to make sure aged animals were able to cope with water restriction and drinking hours (data not shown). Following water-restriction, (iv) the spatial learning task, termed "place learning" was introduced and maintained for 5 days. Here, mice were assigned to their least or second least preferred corner (as recorded in the previous phase and in order to evenly assign corners), meaning that they only had access to water during drinking hours (00-01 am and 05-06 am) in their respective corner. Finally, (v) in the reversal place learning phase (4 days), the corner assignment was switched diagonally for every animal. The first protocol was tested in aged male animals only.

The second IntelliCage protocol again consisted of initial (i) habituation (data not shown) and (ii) nose-poke learning phases (data not shown). No time or place restrictions were used in this protocol and all corners were equal to the animals. In any phase, successfully opened doors automatically closed after 5 s or when the nose-poke area was left. Before the test phases, two sequential training phases were inserted (data not shown): (iii) During training phase 1 the animals learned to trigger yellow LEDs with an initial nose-poke, upon which the next nose-poke opened the door and allowed the animals to drink. Multiple trials could be performed during one visit. The goal of this training phase was to learn the association of yellow light and drinking possibility. (iv) During training phase 2, a delay of 0.5, 1, 2 or 4 s was introduced between the initial nose-poke and the yellow LEDs being turned on, which again indicated drinking possibility by a secondary nose-poke. The individual delay time was randomly assigned every visit and premature nose-pokes had no consequences. (v) Finally, based on the previous training phase, in the first test phase penalties were introduced for premature nose-pokes before the yellow LEDs were on. Premature, incorrect nosepokes triggered blue LEDs and forced the animal to leave the corner in order to be able to start new trials. Also, when the delay time was correctly waited, yellow LEDs went automatically off after 2 s. (vi) Finally, a few adaptations were introduced in the second test phase. The delay time between initial nose-poke and yellow LEDs was fixed to 2 s. However, the duration of the yellow light signals was randomly varied between 0.2, 0.5, 0.8 and 1 s, upon which the animals had to place a correct nose-poke within 2 s. Premature and late nose-pokes again triggered blue light and forced the animals to end the visit before starting new trials. This protocol was tested in separate runs in both female and male aged animals and data was pooled.

Morris Water Maze (MWM)

The Morris Water Maze (MWM) test was performed in a water-filled, black cylindrical tank with a diameter of 123.5 cm. The main experimenter was blinded to the group designation. A non-toxic white dye was mixed into the water in order to hide the submerged platform and make tracking possible for the video tracking software (VideoMot2, TSE Systems, Germany). Extra-maze visual cues with different colors and shapes for orientation were permanently placed on the walls around the tank. The temperature of the water was kept constant at 22 ± 1°C, the test room was illuminated indirectly with diffuse lights and the illumination at the water surface was ~75 lux. The rescue platform had a diameter of 10 cm. The procedure consisted of (i) one day of habituation phase with visible platform (day 0), (ii) four days of training phase with invisible platform (days 1-4) and (iii) a probe trial without a platform 24 h after the last training trial (day 5). Habituation and training phases consisted of four trials per day with 30 min inter-trial interval. In each trial, animals were introduced into the water facing toward the wall of the tank, allowed to swim until they found the platform or for a maximum of 60 s. If the animal found the platform, it was given 10 s for resting and orientation on the platform before it was returned to the cage. During habituation, if the animal did not find the platform, it was put there by the experimenter and was left there for 10 s. If the animal did not find the platform within 60 s on the first training day, it was manually guided to the platform by the experimenter.

At the habituation phase (day 0), the platform was placed 1 cm beneath the water surface but exposed with the help of a colored flag-like sign attached to it. Each of the tested animals were checked at this phase for their eligibility for further testing (accommodation to the task, motivation to escape and intact vision or motor coordination) in four trials, in which the platform and drop locations were changed between each trial (Figure S3A). In the Training Phase the sign was removed, and the platform was placed at the southeast (SE) quadrant, the mice were introduced into the pool from different locations. In the probe trial, the platform was removed, and animals were introduced into the pool at the Northwest starting point and allowed to swim for 60 s. For data analysis, raw xy coordinate data was extracted and analyzed using Microsoft Excel, as the proprietary TSE VideoMot 2 software did not allow some parameters to be extracted. Quality controls like distance to target, total distance and average speed were identical, regardless of the analysis method. The framerate was set to 25 fps and latency to target was calculated by multiplying the frame number by which the mouse had reached the platform by 40 ms. The threshold for a successful target visit (as opposed to an accidental contact) was set to 2 s. For this training parameter, only trials starting from North were considered, as this setup was present in every training session. For animals that did not reach the platform, a 60 s penalty was given. In the probe trial, average distance to target was calculated by averaging the distance of the mouse from each frame to the center of the virtual platform, excluding floating phases. The threshold for floating was set in TSE VideoMot 2 to 1.5 pixel (corresponding to 9.49 cm/s for male trials and 8.61 cm/s for female trials due to slightly different camera positioning).

Time spent in target proximity was assessed by adding up the frames that the mouse resided within a circle around the virtual target platform with a size corresponding to 12.5% of the total pool area (Balschun et al., 2003). Total distance covered was calculated by adding up the distances between the frames. Heatmaps were generated by pooling coordinate raw data of all animals per group. One male mouse from the Control group had to be excluded from analysis during probe trial, because it floated in place during the entirety of the trial.

The probability density maps were made with xy coordinates the kernel density estimate (KDE) plot function of the seaborn data visualization library for Python using a Gaussian kernel and the inferno color map (*kdeplot* settings: kernel = ''gau,'' cbar = True, cmap = ''inferno,'' shade = True, shade_lowest = True).

Open field (OF) test

Prior to the behavioral tests, mice were allowed to adapt to the test room for at least one hour. The OF consisted of an opaque gray plastic box (50 × 50 × 30 cm) and was illuminated by 140 lux at floor level. The ground area of the box was divided into a 36 × 36 cm central area and the surrounding border zone. Mice were individually placed in the center of the OF, and their behavior was tracked during a 5 min test period by a video camera positioned above the center of the OF and recorded with the VideoMot2 software (TSE Systems, Bad Homburg, Germany) (Farzi et al., 2015). The box was cleaned with 70% ethanol between each test trial. Time spent in center, latency to center and total distance were calculated using TSE VideoMot2. Heatmaps were generated as described for the Morris water maze with raw xy coordinate data. The experimenter was blinded to the group designations.

Fly husbandry

Fly stocks were kept on standard Bloomington food at 18°C. During all experiments, flies were maintained at 25°C, 70% humidity and a light/dark cycle of 12h/12h. Agings and crossings were performed on SYA (Bass et al., 2007) (for respirometry) or standard Bloomington food (for memory performance test). Briefly, after 2-3 days of hatching, flies were collected and allowed to mate for 1 day, after which they were transferred to food with or without additional 2 mM SPD. As described previously, for the memory performance test, flies were hatched and aged on food containing 5 mM SPD (Gupta et al., 2013). Agings were performed in small plastic vials á 20 or 30 flies (for respirometry), or large plastic vials á 60-100 flies (for memory performance test) for 10, 20 or 30 days, depending on the experiment. Aging food was changed every 1 – 3 days. Crosses were performed by mating 50 – 100 female virgins with males in a ratio of 10:1.

Fly Memory Performance Test

Olfactory intermediate-term memory (ITM) was performed as described previously (Gupta et al., 2013): 60-100 20-day-old flies (corresponding to 1 technical replicate) were split into 2 portions, transferred to empty plastic vials and allowed to acclimatize in the dark for 30 min. Training and memory trials were performed in a climate chamber (25°C, 65%–70% humidity) under red light (invisible to the flies). Each portion of flies was tapped into a standard T-maze (Tully and Quinn, 1985) and allowed to rest for 2 min. Air flow was set to 2 l/min per maze. Flies were exposed to a conditional olfactory stimulus, either 3-octanol (Sigma-Aldrich #218405, 1:150 in paraffin oil) or 4-methylcyclohexanol (mixture of *cis* and trans, Sigma-Aldrich #153095, 1:55 in paraffin oil) for 1 min, paired with mild electric shocks (12 × 1.25 s pulses of 60 V with 3.75 s intervals in between), followed by a 30 s flush with air. Then, flies were exposed to the other odor for 1 min, followed by another 30 s flush with air. The other portion of flies was trained with the odors switched. Flies were transferred back to empty plastic vials and stored in the dark at room temperature for 3 h. For the memory trials, flies were introduced to the choice point of the T-maze and allowed to choose between the conditional, shock-paired stimulus (CS+) and the non-shocked control stimulus (CS-) for 2 min. The performance index was determined by averaging the performance of each maze (with either 3-octanol or 4-methylcyclohexanol as the CS+), which was calculated by subtracting the number of flies avoiding the CS- from the number of flies avoiding the CS+, divided by the total number of flies. In total, 5 experiments with 3-4 technical replicates each were performed to assess memory performance. While the relative changes between the groups were consistent across

independent experiments, we observed significant variations in absolute ITM performance (inter-experimental variation, p = 0.0390, 42.2% of variation), suggesting that AMI under this experimental setup does not always progress with identical kinetics (see Table S1 for memory performance data of each experiment). Odor avoidance was determined by allowing naive flies to choose between the respective odors or pure air for 2 min (Table S2). Shock avoidance was tested by exposing naive flies to electric shocks and allowing them to escape into the other T-maze arm for 2 min (Table S2).

Quantification of ATP content in fly heads

Tissue preparation

Flies were snap frozen in liquid nitrogen and for each condition 5 heads were collected and 50 μl extraction buffer (acetonitrile:H_2O 2:1) was added. The heads were homogenized for 45 s using a motorized pestle and the homogenate was then centrifuged for 1 min at 20,000 × g at 4°C. To account for variability of the mechanical homogenization, this was done for at least 4 technical replicates per condition and aging experiment. 25 μl of the resulting extract from each technical replicate was pooled and brought to a final volume of 125 μl with extraction buffer. The extracts were stored at −80°C until further analysis.

Reagents

Sodium phosphate, dibasic (Na_2HPO_4), sodium hydroxide, hypochlorous acid (32% m/v), and sodium azide (NaN_3) were obtained from VWR International (Darmstadt, Germany). 3(trimethylsilyl) propionic acid-2,2,3,3-d4 sodium salt (TSP) was obtained from Alfa Aesar (Karlsruhe, Germany). Deuterium oxide (D_2O) was obtained from Cambridge Isotopes laboratories (Tewksbury, MA). Deionized water was purified using inhouse Milli-Q Advantage Water Purification System from Millipore (Schwalbach, Germany). All chemicals were used without further purification. The phosphate NMR buffer solution was prepared by dissolving 5.56 g of anhydrous Na_2HPO_4, 0.4 g of TSP, and 0.2 g NaN_3, in 400 ml of deionized water and adjusted to pH 7.4 with 1M NaOH and HCl. Upon addition of deionized water to a final volume of 500 ml the pH was re-adjusted to pH 7.4 with 1M NaOH and HCl. The buffer was lyophilized and taken up in 500 ml D_2O to obtain NMR buffer in D_2O.

Metabolic quantification using NMR

375 μl of NMR buffer in D_2O were added to the samples containing 125 μl fly head extracts (~10 heads/100 μl) and transferred to 5 mm NMR tubes. All NMR experiments were performed at 310K on an AVANCE Neo Bruker Ultrashield 600 MHz spectrometer equipped with a TXI probe head. The 1D CPMG (Carr-Purcell_Meiboom_Gill) pulse sequence (cpmgpr1d, 512 scans, 73728 points in F1, 11904.76 HZ spectral width, 512 transients, recycle delays 4 s), and a 1D band-selective experiment (selgpse pulse sequence, 512 scans, 73728 points in F1, 11904.76 HZ spectral width, 512 transients, recycle delays 4 s) with water suppression using pre-saturation, was used for 1H 1D NMR experiments. Bruker Topspin version 4.0.2 was used for NMR data acquisition. The spectra for all samples were automatically processed (exponential line broadening of 0.3 Hz), phased, and referenced using TSP at 0.0 ppm using Bruker Topspin 4.0.2 software (Bruker GmbH, Rheinstetten, Germany).

For quantification, processed 1D NMR spectra were imported into MestReNova 11.0 and peaks corresponding to ADP/ATP/AXP signals were integrated. Absolute concentrations were calculated based on integrals of external standards with known concentrations (determined in MestReNova 11.0). Stated concentrations correspond to concentrations in samples per fly head.

Immunoblotting

For protein extraction, lysis buffer (150 mM NaCl, 20 mM Tris/HCl pH 7.5, 1 mM EDTA, 1 mM EGTA, 1% Triton X-100, Phosphatase Inhibitor PhosSTOP Roche #04906837001, HALT Protease Inhibitor Cocktail Thermo Scientific #78439) was added (10 μl/mg tissue wet weight). A motorized pestle was used to homogenize the samples, which were then incubated for 30 min at 4°C with continuous rotation. The homogenized samples were centrifuged for 20 min at 20,000 × g at 4°C. The supernatant was stored at −80°C. Protein concentration was determined by Bradford analysis (BioRad Protein Assay Reagent #500-0006).

30 μg of protein were loaded onto pre-cast polyacrylamide gels (Invitrogen NuPAGE Novex Bis-Tris Gels 12% #NP0343BOX) and run at 100 V. Proteins were transferred to 0.45 μm polyvinylidene fluoride (PVDF) membranes using CAPS buffer (10mM CAPS pH 11, 10% methanol) for 90 min at 220 mA. The blotted membranes were incubated in blocking solution (5 % BSA in TBS [50 mM Tris pH 7.4, 150 mM NaCl]) for one hour and subsequently probed with the respective antibody at room temperature [for α-GAPDH (CST #2118, 1:3000) and α-rabbit-IgG-HRP (CST #7074, 1:3000)] or overnight at 4°C [for α-PKA (CST #4782, 1:1000), α-Phospho-PKA (CST #4781, 1:1000), α-CREB (Abcam ab32515, 1:1000), α-Phospho-CREB (Abcam ab32096, 1:1000), α-CaMKII alpha (Abcam ab103840, 1:1000) and α-Phospho-CaMKII alpha (Abcam ab5683, 1:000)] under shaking conditions. For eIF5A (Beckton-Dickinson BD611976, 1:10000), Hypusine (Merck ABS1064-I, 1:1000), and TFEB (Bethyl Labs A303-673A, 1:1000) antibodies, membranes were blocked with 1% dry milk powder in TBS for 1 hour and probed with the respective antibodies overnight at 4°C. Secondary antibodies were α-rabbit-IgG-HRP and α-mouse-IgG-HRP (Sigma-Aldrich A9044, 1:10000).

All Antibodies were diluted in TST (TBS + 0.1% Tween-20) with 5% BSA. Detection was performed using ECL (Bio-Rad Laboratories) and the ChemiDoc imaging system and data were analyzed and quantified by densitometry with ImageLab software (Bio-Rad laboratories).

High-resolution respirometry

Mice

Oxygen consumption was assayed with an Oxygraph-2k high-resolution respirometer (Oroboros Instruments, Austria) at 37°C according to the manufacturer's recommendations, using a substrate, uncoupler, inhibitor titration ("SUIT") protocol.

Hippocampi were dissected as quickly as possible and samples from the left hemisphere were used for respirometry (while samples from the right hemisphere were subjected to protein extraction).

Samples were homogenized in MiR05 buffer (Gnaiger et al., 2000) (10 μl/100 mg tissue wet weight), filtered through a cell strainer (100 μm) and 10 μl were added to the chamber containing 2 ml equilibrated MiR05 buffer within a closed and calibrated system with constant stirring at 37°C. Measuring complex I activity started with the addition of 5 mM pyruvate and 10 mM glutamate as reduced substrates, which resulted in leak respiration (Leak). The respiratory capacity of mitochondria in an ADP-activated state of oxidative phosphorylation (OXPHOS) was then measured by the addition of 1 mM ADP+Mg^{2+}. 10 μM cytochrome *c* (CytC) were added to test outer mitochondrial membrane integrity. Notably, respiratory rates did not significantly increase upon addition of cytochrome *c* in any of the tested scenarios, confirming an adequate mitochondrial integrity. Maximum OXPHOS capacity was evaluated by adding 10 mM succinate (CI&CII). Titration with carbonyl cyanide 3-chlorophenylhydrazone (CCCP) (2.5 μM steps) assessed maximum respiration in an uncoupled state (ETCmax) and subsequent addition of 5 μM rotenone to assess the maximal ETC capacity supported by complex II alone (CII). Finally, addition of 2.5 μM antimycin A (complex III inhibitor) led to the inhibition of mitochondrial respiratory activity and allowed the evaluation of residual (likely mostly non-mitochondrial) oxygen consumption (ROX). The mice were processed in pairs, one (middle-) aged control combined with one aged SPD-supplemented animal or one (middle-) aged control versus one young animal.

Drosophila

For *Drosophila* samples, flies were immobilized by placing them on ice for about 2 min. Using two precision forceps flies were decapitated and 30 heads were collected on ice. 100 μl of cold MiR05 buffer were added and homogenized for 45 s using a motorized pestle. The homogenate was then filtered through a cell strainer (100 μm) and 20 μl of the suspension were used for high-resolution respirometry. The same SUIT protocol as for mice was used, except for the measuring temperature, which was set to 25°C.

Respirometry data were normalized to total protein content in the respective homogenates, determined by Bradford analysis. To minimize background signal of the BSA present in the extraction buffer, samples were diluted 1:10 in ultra-pure H_2O and diluted extraction buffer was used for background correction.

Epidemiological Analyses

Characteristics

As detailed previously (Eisenberg et al., 2016; Kiechl et al., 2013; Stegemann et al., 2014; Willeit et al., 2014), participants were carefully evaluated regarding their medical history, life-style behaviors, and vascular risk factors using standardized questionnaires and protocols. Individuals were coded as current smokers or non-smokers (including former smokers). Alcohol intake was quantified in grams per day. Body mass index was calculated as weight in kilograms divided by height squared in meters. Systolic and diastolic blood pressures were taken after the participant had been sitting for at least ten min, and the mean of three independent measurements was calculated. Hypertension was defined as systolic blood pressure $\geq$ 140 mmHg or diastolic blood pressure $\geq$ 90 mmHg or the use of antihypertensive drugs. Blood samples were taken in the morning hours after an overnight fast and 12 hours of abstinence from smoking and immediately processed or stored at −70°C. Diabetes mellitus was diagnosed when fasting plasma glucose exceeded 126 mg/dl or when participants were on anti-diabetic medication. Three categories of socioeconomic status (low, medium, high) were defined based on information about occupational status and educational level of the person with the highest income in the household. We quantified physical activity by means of the Baecke questionnaire (Baecke et al., 1982), rated activity intensities according to the compendium of physical activities (Ainsworth et al., 2000), and used these data to calculate average metabolic-equivalent hours (MET-hours) per week as a measure of long-term physical activity. Total energy expenditure was estimated by multiplying the resting energy expenditure derived from age, sex, weight, and height (Mifflin et al., 1990) by a value reflecting the physical activity level of each participant's profession (FAO/WHO/UNU Expert Consultation, 2005) and adding calories burnt through sport and leisure-time activity derived from the Baecke questionnaire.

Dietary assessment

Dietary intake was evaluated by quinquennial 118-item food-frequency questionnaires (FFQ) based on the gold-standard FFQ by Willett and Stampfer (Willett et al., 1985) and adapted to the dietary peculiarities in the survey area. FFQs were administered by dieticians, a unique procedure that ensures high data quality, and dieticians made use of illustrative photos of foods when exploring aphasic patients and of information provided by spouses, caregivers, and nursing homes. For each item in the FFQ, a common unit or portion size was specified, and we instructed participants to customize how often on average they had consumed that amount in the past five years. The nine response categories ranged from 'never' to 'six or more times a day'. We calculated nutritional intake by assigning a weight proportional to the frequency of use for each food (e.g., once per day equals a weight of one), multiplying this weight by the nutrient value for the specified portion size, and summing the contribution of all foods. We dissected complex foods into component foods utilizing common recipes. Nutrient composition data for foods were based on the US Department of Agriculture Nutrient Database (Release 23) (Gebhardt et al., 2010). We compiled a special nutrient database for polyamines consistent with our FFQ (Kiechl et al., 2018). Estimates of polyamines and intake of other nutrients were calorie-adjusted. For that purpose, we used

the residuals obtained by regressing polyamine or other nutrient intake on total energy intake (Willett and Stampfer, 1986). Reproducibility and validity of the original FFQ are well documented (Willett et al., 1985) and extend to its application in the Bruneck Study. Dietary patterns remained stable over time. Accordingly, under most circumstances point estimates adequately reflect medium-term dietary intake. A comparison with nine-day diet records shows a high level of agreement - overall and with regards to polyamine intake (Kiechl et al., 2018). From a technical perspective, our study ranks among those providing highest quality in the nutritional epidemiology field.

We calculated the ratio of calorie intake to energy expenditure further on termed 'caloric ratio'. This ratio reflects caloric excess or restriction - one of few dietary features convincingly linked to healthspan and probably lifespan in humans.

The average daily glycemic load was calculated according to Atkinson et al. (2008) by multiplying each food item's glycemic index by the respective carbohydrate content and summing up the results for all food items (Brand-Miller et al., 2009; Liu et al., 2000). The Alternate Healthy Eating Index (AHEI), a measure of diet quality, significantly associated with the risk of major chronic diseases in a large number of studies, was calculated as described previously (McCullough et al., 2002). We did not consider the 'duration of multivitamin use' because multivitamin supplementation was almost absent in our cohort.

Ascertainment of cognitive function

Global cognitive function was assessed by quinquennial Mini Mental State Examinations (MMSEs) (Folstein et al., 1975), Cambridge Examination for Mental Disorders of the Elderly (CAMDEX) screening questions on memory deficits (subjective memory impairment) (Roth et al., 1986), and thorough neuropsychiatric examinations with application of the Diagnostic and Statistical Manual of the Mental Disorders, fourth edition (DSM-IV) (Guze, 1995) clinical criteria for dementia and depression. We also included a careful review of the reports of all medical visits and examinations ever made on study participants as part of routine clinical care (i.e., outside the study protocol). The situation in Bruneck is unique in that (i) the only specialists in neurology and psychiatry and the only radiological department offering CT/MRT are located at the Bruneck Hospital, (ii) all reports were available for review, and (iii) population mobility in the survey area was low over the last decade (< 0.2% per year).

DSM-IV criteria for the diagnosis of dementia are as follows (all four criteria must apply): A. The development of multiple cognitive deficits manifested by both memory impairment and one or more of the following: aphasia, apraxia, agnosia, and disturbance in executive functioning. B. The cognitive deficits cause significant impairment in social or occupational functioning and represent a significant decline from a previous level of functioning. C. The deficits do not occur exclusively during the course of a delirium. D. The disturbance is not better accounted for by another axis I disorder (e.g., major depressive episode, schizophrenia).

The MMSE is the best established screening test for dementia with a sensitivity and specificity of 0.81 and 0.89, and for cognitive impairment as well (Tsoi et al., 2015). MMSEs were corrected for age, sex, and education years and transformed to z-scores using CERAD Plus 1.0 based on a comparison to a normal population from Basel (n = 1100, age range 49 to 92 years) (Welsh et al., 1994). A z-score of 0 represents a cognitive performance equal to the healthy normal population, while low values indicate cognitive impairments.

In 2000, cognitive assessment in the Bruneck Study cohort was supplemented by the Consortium to Establish a Registry for Alzheimer's Disease (CERAD) (Morris et al., 1989; Welsh et al., 1994) cognitive test battery in the event of subjective memory complaints (CAMDEX) and/or a MMSE z-scores < -1.03 (i.e., 15th percentile as recommended by the CERAD 1.0). CERAD involved the Word List – Savings, Word List – Retrieval, Word List – Retention, Category Fluency (Animals), Boston Naming Test, Figures – Copy, Figures – Delayed Recall, Figures – Savings, Trail Making Test Part A, and Trail Making Test Part B. The individual tests were combined to the three domains memory (Word List – Savings, Retrieval, and Retention), attention and executive functioning (Trail Making Test Part A and B), and language (Boston Naming Test, Category Fluency (Animals), and Phonematic Fluency) by computing averages of the individual z-scores (Mapstone et al., 2014). A composite cumulative impairment score (ranging from 0 to 3) was constructed as the sum of the three domain scorings (a score of 1 was given for each domain z-score < -1.03). Normal cognition was defined by a MMSE z-scores ≥ -1.03, no subjective memory complaints (CAMDEX), and no DSM-IV diagnosis of dementia (neuropsychiatric examination and review of hospital records). In case of subjective memory complaints (CAMDEX) and/or a MMSE z-scores < -1.03, results of the CERAD were decisive and domain z-scores < -1.03 were considered as indicative of cognitive impairment as were MMSE z-scores < -1.96 (i.e., 2.5th percentile) or a diagnosis of dementia according to DSM-IV criteria.

QUANTIFICATION AND STATISTICAL ANALYSIS

Data are presented either as line graphs showing means ± SEM or as boxplots, showing median (center line) and interquartile ranges (IQR), along with whiskers showing minima and maxima. Sample size (indicated in brackets in figures) always refers to biological replicates (individual animals) in mice or independent aging experiments in flies. Statistical testing was performed using Graphpad Prism 9®. Student's t test (paired or unpaired, as appropriate) and analysis of variance (ANOVA) with Tukey's or Dunnett's post hoc tests were used for comparisons between two or multiple groups, respectively. Overall normal distribution of data was confirmed by Shapiro-Wilk test and/or visual inspection of QQ-plots of residuals. In case of normality violation, Mann-Whitney U-test was used for comparison of two groups and Kruskal-Wallis test with Dunn's correction for three groups, respectively. Where appropriate, a two-way ANOVA was applied, followed by testing simple main effects in case of main-factor or interaction significance. For mouse learning performance, a repeated-measure mixed model ANOVA with time (within subjects factor) and treatment (between subjects

factor) as independent factors was applied. Sphericity was tested using OriginPro 8®. In case of sphericity violations, the Geisser-Greenhouse correction was applied. The reported significance values are always two-sided.

For epidemiological data, logistic regression analysis was used to estimate odds ratios (ORs) and 95% confidence intervals (95% CIs) for the association between baseline SPD intake (1995) and cognitive impairment assessed as part of the 2000 evaluation (see section Ascertainment of cognitive function). This analysis was confined to study participants with normal baseline (1995) cognition. All analyses were adjusted for age, sex, and the 'caloric ratio'. Multivariable analyses additionally controlled for social status, level of physical activity, alcohol consumption, body-mass index, smoking, diabetes, hypertension, and aspirin medication. We modeled polyamine intake as a continuous variable (after $\log_e$-transformation) and documented a linear dose-response type of association using SPD categories (tertile groups). We did not update SPD intake during follow-up because cognitive status may well affect dietary habits (potential of reverse causation). To substantiate our findings, sensitivity analyses (a) exclude individuals with major depression potentially interfering with cognitive function testing and (b) additionally adjust for composite categories of food items (calorie-adjusted intake of red/processed meat, vegetables/fruits, and dairy products) or for the Alternate Healthy Eating Index to minimize the potential of confounding by healthy diet and life-style. Because SPD intake is presumably part of a healthy diet, this analysis is expected to yield conservative risk estimates. All P values are two-sided. Analyses were conducted using R 3.2.2 (R Foundation for Statistical Computing, Vienna, Austria) and SPSS 22.